ENHANCING ANTICANCER EFFICACY OF LIPOSOMAL DOXORUBICIN BY MODULATION OF TUMOR MICROENVIRONMENT AND PREPARATION OF STABLE LIPOSOMES

A DISSERTATION
SUBMITTED TO THE DEPARTMENT OF DRUG DELIVERY RESEARCH
GRADUATE SCHOOL OF PHARMACEUTICAL SCIENCES
HOSHI UNIVERSITY
IN PARTIAL FULFILLMENT OF THE REQUIREMENTS
FOR THE DEGREE OF
DOCTOR OF PHILOSOPHY IN PHARMACEUTICAL SCIENCES

ANDANG MIATMOKO

March, 2017

学位論文　(博士)

ENHANCING ANTICANCER EFFICACY OF LIPOSOMAL DOXORUBICIN BY MODULATION OF TUMOR MICROENVIRONMENT AND PREPARATION OF STABLE LIPOSOMES

2017年3月

星薬科大学大学院　薬学研究科

総合薬科学専攻

医療薬剤学

ANDANG MIATMOKO

TABLE OF CONTENTS

General Introduction **1**

Chapter 1

Zoledronic acid could enhance antitumor efficacy of liposomal doxorubicin 8

I. Introduction 9

II. Materials and Methods 11

2.1. Materials 11

2.2. Cell culture 11

2.3. Tumor model 11

2.4. Immunohistochemical analysis 12

2.5. IFP measurement in tumors 12

2.6. Determination of serum cytokine levels 13

2.7. Quantitative real-time PCR 13

2.8. Cytotoxicity 14

2.9. *In vivo* therapeutic studies 14

2.10. Biodistribution of DOX 15

2.11. Statistical analysis 15

III. Results 16

3.1. Vascular structure of tumor after treatment with ZOL 16

3.2. Change of IFP 18

3.3. Change of macrophages in tumor and cytokine levels in serum after ZOL treatments 19

3.4. *In vitro* antitumor effect 22

3.5. Antitumor effect on LLC tumor-bearing mice 22

3.6. Accumulation of DOX liposomes in tumor 25

IV. Discussion 26

Chapter 2

Tumor delivery of liposomal doxorubicin prepared with poly-L-glutamic acid as a drug trapping agent 30

I. Introduction 31

II. Materials and Methods 33

2.1. Materials 33

2.2. Preparation of liposomes 33
2.3. Measurement of particle size and ζ-potential of liposomes 34
2.4. Evaluation of DOX/PGA complex formation 34
2.5. Small angle X-ray diffraction (SAXRD) analysis of liposomal DOX 35
2.6. *In vitro* doxorubicin release from DOX/PGA aggregate and liposomal DOX 35
2.7. *In vitro* cytotoxic assay of liposomes 36
2.8. Antitumor activity of liposomal DOX 36
2.9. Biodistribution of liposomal DOX 37
2.10. Statistical analysis 37
III. Results 38
3.1. Preparation and characterization of liposomal DOX using PGA 38
3.2. Evaluation of DOX-PGA complex formation 39
3.3. Small angle X-ray diffractions (SAXRD) analysis of liposomal DOX 41
3.4. Evaluation of *in vitro* DOX released from DOX-PGA aggregates 42
3.5. The effect of PGA on drug release from liposomes 43
3.6. *In vitro* cytotoxic assay of liposomes 44
3.7. Antitumor activity of liposomal DOX 46
3.8. Biodistribution of liposomal DOX 47
IV. Discussion 48
Conclusion 51
Acknowledgments 54
References 55

LISTS OF TABLE AND FIGURES

General Introduction

Figure 1 3
Figure 2 4
Figure 3 5
Figure 4 7

Chapter 1 Zoledronic acid could enhance antitumor efficacy of liposomal doxorubicin

Figure 5 17
Figure 6 19
Figure 7 20
Figure 8 21
Figure 9 23
Figure 10 24
Figure 11 25

Chapter 2 Tumor delivery of liposomal doxorubicin prepared with poly-L-glutamic acid as a drug trapping agent

Table 1 40
Figure 12 41
Figure 13 42
Figure 14 43
Figure 15 44
Figure 16 45
Figure 17 46
Figure 18 47

LISTS OF ABBREVIATIONS

ANOVA	analysis of variance
APR	acute-phase response
CD31	cluster of differentiation 31
cDNA	complementary deoxyribonucleic acid
Chol	cholesterol
DOX	doxorubicin
EPR	enhanced permeability and retention
FDA	food and drug administration
FBS	fetal bovine serum
GAPDH	glyceraldehyde-3-phosphate dehydrogenase
gDNA	genomic deoxyribonucleic acid
GM-CSF	granulocyte-macrophage colony-stimulating factor
HSPC	hydrogenated soya phosphatidylcholine
HPLC	high performance liquid chromatography
IFN-γ	interferon gamma
IFP	interstitial fluid pressure
IL	interleukin
LLC	Lewis lung carcinoma
MMP-9	matrix metalloproteinase-9
mPEG-DSPE	methoxy-(polyethylene-glycol)-distearylphosphatidylethanolamine
MWCO	molecular weight cut-off
PBS	phosphate-buffered saline
PECAM	platelet endothelial cell adhesion molecule
PEG	polyethylene glycol
PGA	poly-α,L-glutamic acid
pKa	logarithmic scale of acid dissociation constant
RT-PCR	reverse transcription-polymerase chain reaction
RES	reticulo-endothelial system
mRNA	messenger ribonucleic acid
SAXRD	small angle X-ray diffraction
α-SMA	smooth muscle alpha-actin
TAMs	tumor-associated macrophages

TEA	triethylamine
TGF-β	transforming growth factor beta
T_m	transition temperature
TNF	tumor necrosis factor
VEGF	vascular endothelial growth factor
ZOL	zoledronic acid

LIST OF PUBLICATIONS

Dissertation drafts:

1) Zoledronic acid enhances antitumor efficacy of liposomal doxorubicin.: Y. Hattori, K. Shibuya, K. Kojima, A. Miatmoko, K. Kawano, K. Ozaki, E. Yonemochi, Int. J. Oncol., 47, 211-219 (2015): **Chapter 1**

2) Tumor delivery of liposomal doxorubicin prepared with poly-L-glutamic acid as a drug-trapping agent.: A. Miatmoko, K. Kawano, H. Yoda, E. Yonemochi, Y. Hattori. J. Liposome Res, in press (2016): **Chapter 2**

Other publications:

1) Evaluation of cisplatin-loaded polymeric micelles and hybrid nanoparticles containing poly(ethylene oxide)-block-poly(methacrylic acid) on tumor delivery. A. Miatmoko, K. Kawano, E. Yonemochi, Y. Hattori. Pharmacology & Pharmacy, 7, 1-8 (2016).

2) Evaluation of transfersome and protransfersome for percutaneous delivery of cisplatin in hairless mice. A. Miatmoko, K. Kawano, Y. Hattori, Y. Maitani, E. Yonemochi. J. Pharmaceu. Pharmacol., S(1), 7 (2015).

GENERAL INTRODUCTION

Cancer cells are genetically malignant transformed cells that enormously grow, could evade suicidal apoptotic program, and invade or metastasize to healthy tissues or organs.[1)] These alterations occurred because of unhealthy diets and obesity, little physical exercise, tobacco, infectious agents, and environmental carcinogens, etc.[2)] The uncontrolled cell proliferation in cancer can lead to formation of abnormal cell mass called tumor.[3)]

Surgery, radiotherapy, chemotherapy, and their combinations have been widely used for cancer treatment.[4)] Chemotherapy becomes an effective treatment for cancer, even for metastatic cancer spread throughout the body,[5–7)] since it could be delivered *via* blood circulation by which the drugs could reach tumor sites in tissues or organs in the body.[8)] On the other hand, conventional chemotherapy has many limitations on its use. It often produces no tumor-specific delivery resulted in wide drug distribution in the whole body. As the results, healthy cells become damaged and drugs are rapidly cleared due to metabolism and excretion. Therefore, drug concentrations are mostly found to be low and ineffective to kill cancer cells in tumor. Increasing the dose of drugs could not be a proper therapy option because it will raise the risks of healthy organs being exposed to more drugs and suffered from undesired toxic effects.

Recently, nanoparticles have been widely investigated as innovative tools for solving the vulnerability in chemotherapy. It can effectively deliver anticancer drugs to tumor *via* an enhanced permeation and retention (EPR) effect. This phenomenon is related to the abnormal anatomy of tumor vasculatures. When tumor grows larger, the normal vasculatures could not sufficiently provide any nutrients for tumor growth and expansion.[9)] Therefore, cancer cells will secrete angiogenic growth factors such as vascular endothelial growth factors (VEGF) that triggers neovascularization. The development of tumor neovasculatures results in

abnormalities on the structures and barrier functions of blood microvessels. Tumor blood vessels are absent in pericyte coverage, and have defects in endothelial monolayer arrangement, which cause intercellular gaps and large opening of vessel walls.[10] Therefore, these vessels are leaky, losing their normal barriers function. They become hyperpermeable to large molecules, including nanoparticles. In addition, impaired networks of lymphatic vessels in tumor reduces the clearance of these nanoparticles from tumor tissue.[11] As the consequences, nanoparticles are able to extravasate into tumor interstitium and they are retained there, manifesting in high accumulation of nanoparticles in tumor.[12]

Among many types of nanocarriers, liposome offers a superior form for drug delivery. Liposome is a colloidal particle composed of biocompatible lipid bilayer, which surrounds an inner water phase, thus providing complete protection for drugs entrapped inside.[13] Liposome has favorable properties such as offering formulations with desirable composition, size, surface charge, ability to encapsulate both hydrophilic and hydrophobic materials with high efficiency, and the possibility for efficient surface functionalization with specific ligands.[14] Polyethylene glycol (PEG) modification (PEGylation) of liposome enables prolonged drug circulation in the bloodstream because of its ability to form an aqueous "mask" layer on liposomal surface.[15] It prevents adsorption of serum proteins, thus reducing liposome uptake by reticuloendothelial system (RES). Taking the advantages of the EPR effect, PEG-modified liposome can be highly accumulated in tumor.[16]

Liposome has been known as the most developed and established injectable nanocarriers approved by FDA for delivery of doxorubicin (DOX), such as Doxil®/Caelyx®, Lipodox®, and DOX-NP™.[17] DOX is an anthracycline compound (Fig. 1) that is widely used for treatments of breast cancer, lymphomas and many solid tumors,[18,19] but its effect is often limited by the potential side effects of cardiomyopathy, etc.[20] It has been reported that encapsulation of DOX into PEGylated liposome provides great advantages, especially for the

reduction of DOX-related cardiotoxicity.[4,21] Since liposome could provide stable DOX encapsulation, the free DOX amount could be decreased during distribution in systemic circulation, thus reducing its toxicities.

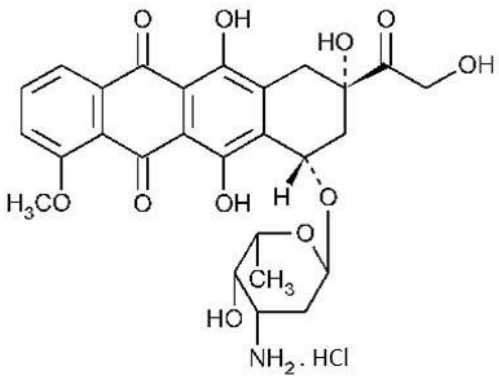

Figure 1. The chemical structure of DOX hydrochloride.

There are some limiting steps for liposome to successfully reach cancer cells and produce antitumor activity, which include drug circulation in blood, vessel extravasation, penetration in tumor tissue, and drug release inside the cells.[22] Although liposome accumulation highly depends on the EPR effect, the heterogeneous nature of tumor microenvironment contrarily limit tumor drug delivery (Fig. 2). Not only does the leaky tumor neovasculatures facilitate extravasation of liposome, but it also permits macromolecules such as proteins to penetrate into interstitial tumor space. Because of defective draining system of lymphatic vessel in tumor tissue, large accumulation of these macromolecules can lead to an increase of interstitial fluid pressure (IFP) in tumor.[23] The increase of IFP induces an outward convective flow, which limits further tumor extravasation and deep penetration of liposome. In addition, the heterogeneity of tumor vascularization often results in different liposome distribution within tumor region, where well vascularized area shows better liposome accumulation than limited or non-vascularized area.[24] These barriers hamper tissue penetration and molecular movement of the distant liposome to reach

cancer cells,[25] thus producing insufficient drug concentrations and causing failure in cancer therapy.[26]

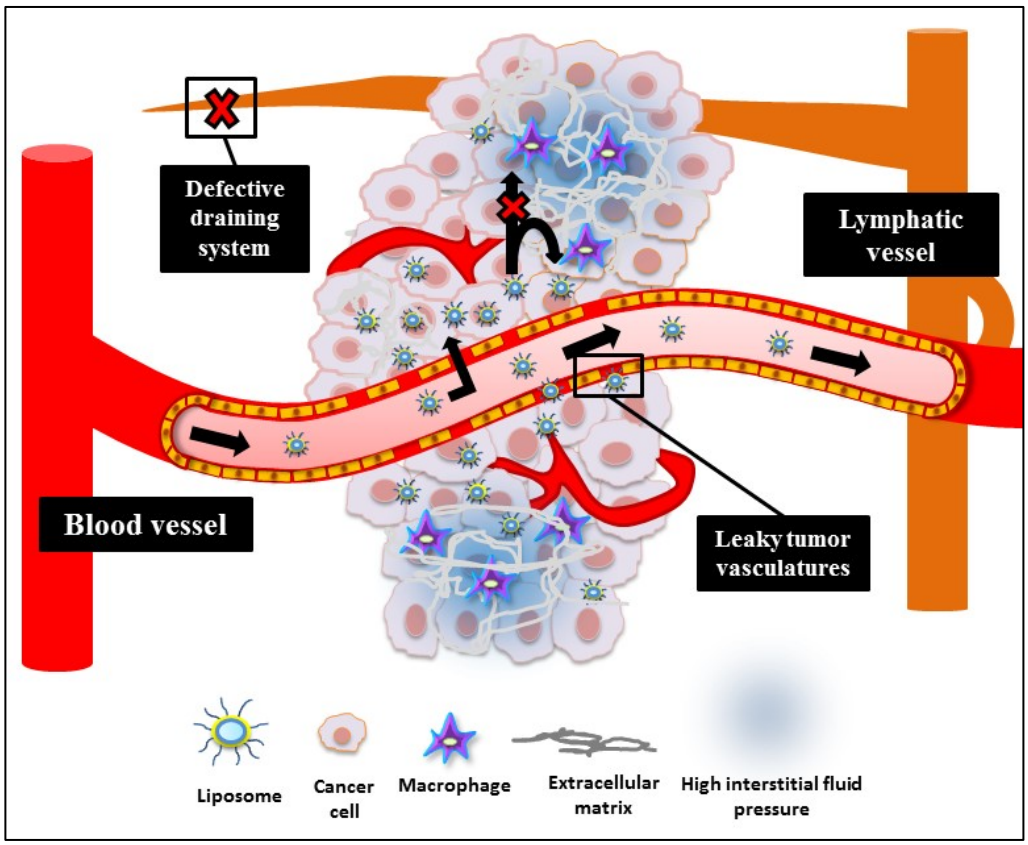

Figure 2. Schematic representation of delivery of liposomes in tumor.

To improve tumor delivery of liposome, the limitations on the EPR effect should be successfully resolved. Since liposome is delivered through blood circulation, modulation of tumor microenvironment focusing on tumor vascularization may increase the amount of liposome penetrated and distributed in tumor tissue. It has been known that antiangiogenesis therapy has evidences to change tumor vasculatures and this therapy becomes a complementary therapeutic paradigm for cancer.[27,28] Preclinical studies have shown that anti-VEGF therapy changes the tumor vasculatures toward a more mature or normal phenotype.[9] Normalization of disorganized tumor vasculatures using therapeutics reduces tumor hypoxia,

IFP, and hyperpermeability. Therefore, normalizing tumor vasculatures may overcome the physiological barriers and generate obvious blood flow facilitating the delivery of liposome to tumor.[29)]

Tumor-associated macrophages (TAMs) are abundant immunosuppressive cells recruited into tumor microenvironment by cytokines such as macrophage colony-stimulating factor (M-CSF).[30,31)] The relevance of TAMs to tumor progression and metastasis is well established. These cells express angiogenic promoters, such as vascular endothelial growth factor (VEGF) that triggers cell cycle progression on endothelial cells promoting tumor neovascularization.[32–34)] Therefore, TAMs are potential target for antiangiogenic therapy. Zoledronic acid (ZOL), which is a nitrogen-containing bisphosphonate compound (Fig. 3),[35,36)] can become an agent for selective depletion of TAMs. ZOL is a highly charged hydrophilic molecule that does not readily cross the plasma cell membrane, thus showing pharmacological activity only in cells that exhibit fluid-phase endocytosis, such as macrophages.[37,38)] Depleting TAMs will reduce tumor VEGF levels that affect tumor vascularization, thus providing benefits for tumor drug delivery.

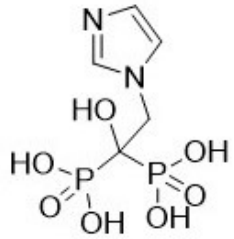

Figure 3. The chemical structure of ZOL.

In addition to the modulation of tumor microenvironments as described above, modification of liposomal DOX formulation can also be an approach to improve delivery of drug to tumor. Stable liposome will be useful to avoid DOX loss, achieve prolonged

circulation time, and improve DOX delivery to tumor by the EPR effect,[11,39] thus altering the biodistribution and antitumor activity of DOX.

In the case of DOXIL®, which is the marketed product of liposomal DOX, the use of hydrogenated soybean phosphatidylcholine (HSPC) that has high phase transition temperature (T_m) in combination with cholesterol produce its stable liposomal membrane.[40] Furthermore, the transmembrane gradient of ammonium sulfate (AS) generates high drug loading and retention of DOX through the formation of DOX-sulfate rod-like aggregates in the liposomal interior because of the over solubility limits of DOX and its interaction with sulfate ions.[41] However, these intrinsic stabilities restrict DOX release resulting in an insufficient biologically active DOX amount in cancer cells although DOXIL® is highly accumulated in tumor.[42] Therefore, modification of such intraliposomal DOX stabilization may provide an alternative solution to modify DOX release from liposome, which makes liposomal DOX rigid and stable in blood circulation, but releases DOX soon once it reaches tumor tissue.

Generally, intraliposomal drug stabilization can be achieved through the formation of stable drug complexes,[43–46] or physical aggregate-like compounds in water.[47–49] To modify drug restraint against diffusion, an appropriate drug trapping agent could be used to effectively control both drug loading and drug release. Poly-α,L-glutamic acid (PGA) is a synthetic polyamino acid that consists of glutamic acid monomer units with large number of carboxyl groups (Fig. 4). PGA has an apparent pKa of 5.4,[50] where at around pH 7, PGA will be ionized providing functional binding sites for cationic drugs. It has been reported that the ionic interactions between poly-γ-glutamic acid and DOX produced random colloidal aggregates and sustained DOX release.[51] Therefore, PGA may be favorable as a trapping agent for tumor delivery of liposomal DOX.

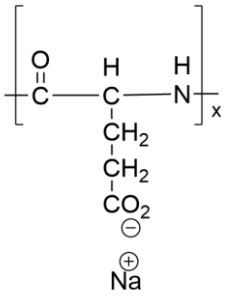

Figure 4. The chemical structure of PGA.

This study aimed to investigate methods for improving antitumor efficacy of DOX by using two approaches, firstly, *via* modulation of tumor microenvironment, and secondly, by preparation of stable liposomes. In Chapter 1, I investigated whether ZOL treatment could affect tumor vascularization and further evaluated TAMs depletion used as the first approach to improve delivery of liposomal DOX. In Chapter 2, I studied preparation of stable liposomes as the second approach, which focused on the use of PGA as an intraliposomal trapping agent for tumor delivery of DOX.

Chapter 1

Zoledronic acid could enhance antitumor efficacy of liposomal doxorubicin

I. INTRODUCTION

Tumor microenvironment, which involves the complex interactions among cancer cells, normal cells, immune-derived cells, lymphatic and blood vessels surrounding and feeding cancer cells,[3,52] has created challenges for delivery of drug in tumor. Although the EPR effect has been known to allow liposomes for preferably accumulating in tumor, the abnormalities of tumor neovasculatures and impaired network of lymphatic vessels, which are important factors that establish the EPR phenomenon, contrarily cause poor tumoral distribution of liposomal drug.[23,53] Therefore, managing these tumor microenvironments would give advantages to improve tumor drug delivery. It has been observed that transforming growth factor (TGF)-β type I receptor inhibitors increased the antitumor effect of liposomal DOX or micelle DOX by changing the microenvironment of the vasculatures.[54,55]

Antiangiogenesis treatments that could restore the balance between pro- and antiangiogenic cytokines in tumor tissue showed evidence for remodeling tumor vasculatures toward more mature or normal phenotype to improve delivery of chemotherapeutics.[56] VEGF inhibitors or anti-VEGF antibody treatment reduced tumor hypoxia, IFP, and hyperpermeability of tumor vasculatures. Since TAMs express VEGF and promote angiogenesis, depletion of TAMs may become a way for normalizing tumor vascularization and modulating the tumor microenvironment.

Recent study showed that ZOL produced toxic effects to RAW264.7 macrophage cells and the intravenous injections of ZOL solution into mice bearing tumor could induce the change of vascular structure in tumor;[57] however the mechanism is still unclear. Due to its selective uptake by macrophages, ZOL treatment may target TAMs depletion that affects VEGF levels required for tumor neovascularization, thus providing benefits for tumor drug delivery.

In this chapter, ZOL treatment has been evaluated whether it could facilitate the delivery of liposomal DOX (Doxil®) by changing the microenvironment of the vasculatures and increase the therapeutic efficacy *in vivo*.

II. MATERIALS AND METHODS

2.1 Materials

Zoledronic acid (ZOL) was obtained from Enzo Life Sciences (Farmingdale, NY, USA). Doxorubicin hydrochloride (DOX) was purchased from Wako Pure Chemical Industries Inc. (Osaka, Japan). Liposomal DOX, Doxil®, was obtained from Janssen Pharmaceutical K.K. (Tokyo, Japan). All other chemicals were of the finest grade available.

2.2 Cell culture

Murine Lewis lung carcinoma (LLC) was obtained from the Cell Resource Center for Biomedical Research, Tohoku University (Miyagi, Japan). Murine macrophage RAW264.7 was obtained from the European Collection of Cell Cultures (ECACC, Wiltshire, U.K.). LLC and RAW264.7 cells were cultured in RPMI-1640 medium with 10% heat-inactivated fetal bovine serum (FBS) and kanamycin (100 μg/ml) in a humidified atmosphere containing 5% CO_2 at 37˚C.

2.3 Tumor model

All animal experiments were performed with approval from the Institutional Animal Care and Use Committee of Hoshi University, which is accredited by the Japanese Ministry of Education, Science, Sports and Culture. For the generation of LLC tumors, 1 x 10^6 cells suspended in 100 μL of PBS pH 7.4 were inoculated subcutaneously into the flank of female C57BL/6N mice (Sankyo Labo Service Corp.). The tumor volume was calculated using the following formula: tumor volume = 0.5 x a x b^2, where a and b are the larger and smaller diameters, respectively.

2.4 Immunohistochemical analysis

To examine the antiangiogenic effect of ZOL on tumor, ZOL solution was intravenously injected at a dose of 5, 20 or 40 μg of ZOL/mouse per day for one, two or three consecutive days into mice bearing LLC tumor when the tumor volume reached approximately 200 mm^3. The tumors 24 h after the final injection of ZOL solution were frozen on dry ice and sliced at 16 μm. Their sections were incubated with rat anti-mouse CD31 (PECAM-1) monoclonal antibody (Clone MEC 13.3, BD Pharmingen, San Diego, CA, USA) for the detection of mouse endothelial cells, and subsequently incubated with goat anti-rat IgG conjugated to Alexa Fluor 488 (Invitrogen, Carlsbad, CA, USA) as a secondary antibody. In the detection of mouse pericytes, the sections were further incubated with Cy3-conjugated rabbit anti-smooth muscle α-actin (α-SMA) antibody (Sigma-Aldrich, MO, USA).

To examine the effect of ZOL on macrophages in tumor and liver, ZOL solution was injected intravenously at a dose of 40 μg of ZOL/mouse per day for three consecutive days into mice bearing LLC tumor. The sections of tumor and liver 24 h after the final injection of ZOL solution were incubated with rat anti-mouse F4/80 monoclonal antibody (Clone CI:A3-1, AbDSerotec, Oxford, UK) for the detection of mouse macrophages, and subsequently incubated with goat anti-rat IgG conjugated to Alexa Fluor 488 as a secondary antibody. Immunofluorescence was examined microscopically using an ECLIPSE TS100-F microscope (Nikon, Tokyo, Japan).

2.5 IFP measurement in tumors

When the tumor volume reached approximately 150 mm^3, LLC tumor-bearing mice were intravenously injected with ZOL solution at a dose of 5, 20 or 40 μg of ZOL/mouse per day for three consecutive days. Twenty-four hours after the final injection of ZOL solution, the mice were anesthetized with isoflurane, and then IFP of tumors was measured with a

needle probe pressure monitor, fitted with an 18-gauge side-ported needle (Intra-Compartmental Pressure Monitor System; Stryker, Kalamazoo, MI, USA) connected to a syringe filled with 0.9% saline, as previously reported.[58] The needle probe was inserted into the center of the tumor or normal muscle, and IFP was recorded. The IFP in tumors was normalized to that in muscle.

$$Normalized\ IFP = \frac{\text{IFP (mmHg)of tumor}}{\text{IFP (mmHg)of muscle}}$$

2.6 Determination of serum cytokine levels

When the tumor volume reached approximately 150 mm^3, LLC tumor-bearing mice were intravenously injected with ZOL solution at a dose of 40 μg of ZOL/mouse per day for three consecutive days. Twenty-four hours after the final injection of ZOL solution, serum was prepared by separation of the coagulated whole blood. Serum cytokine levels, including interleukin (IL)-10 and -12 (p70), granulocyte-macrophage colony-stimulating factor (GM-CSF) and tumor necrosis factor (TNF)-α, were determined using mouse cytokine Th1/Th2 Panel (Bio-Rad, Hercules, CA) and Bio-Plex 200 system (Bio-Rad). Normal values were determined using blood obtained from age-matched, normal mice without LLC tumor.

2.7 Quantitative real-time PCR

When the tumor volume reached approximately 200 mm^3, LLC tumor -bearing mice were intravenously injected with ZOL solution at a dose of 40 μg of ZOL/mouse per day for three consecutive days. For the expression level of VEGF mRNA in tumor tissues, the tumors were excised from LLC tumor-bearing mice 24 h after the final injection of ZOL solution, and then total RNA was isolated from the tumors using the TRI Reagent (Molecular Research Center, Inc., Cincinnati, OH, USA). RNA yield and purity were checked by spectrometric measurements at 260 and 280 nm. cDNA was synthesized from

total RNA by using the PrimeScript RT Reagent Kit with gDNA Eraser (Takara Bio Inc., Shiga, Japan). Quantitative real-time PCR was performed with the Takara Thermal Cycler Dice (Takara Bio Inc.) and TaqMan Gene expression assays (vegfa: Mm00437306_m1, gapdh: Mm99999915_g1; Applied Biosystems®, CA, USA). Samples were run in triplicate and the expression levels of VEGF mRNA were normalized for the amount of glyceraldehyde-3-phosphate dehydrogenase (GAPDH) mRNA in the same sample, and analyzed using the comparative Ct method.

2.8 Cytotoxicity

LLC and RAW264.7 cells were seeded separately at a density of 1 x 10^4 cells per well in 96-well plates and maintained in RPMI-1640 medium supplemented with 10% FBS for 24 h before treatment. To examine cytotoxicity for ZOL, LLC and RAW 264.7 cells were treated with medium containing from 2.5 to 40 μM ZOL, and they were then incubated for 48 h. To examine the effect of ZOL on the cytotoxicity of DOX, LLC and RAW 264.7 cells were treated with medium containing from 0.125 to 2 μM DOX in the presence or absence of 20 μM ZOL, and they were then incubated for 48 h. The cell number was determined with Cell Counting Kit-8 (Dojindo Laboratories, Kumamoto, Japan). Cell viability is expressed relative to the absorbance at 450 nm of untreated cells.

2.9 *In vivo* therapeutic studies

When the average volume of the tumors reached 100-200 mm^3 in mice bearing LLC tumors, ZOL solution was intravenously administered *via* lateral tail veins at a dose of 40 μg of ZOL/mouse on days 0, 1 and 2, and then Doxil® was intravenously administered at a dose of 5 mg of DOX/kg on day 3. Tumor volume and body weight were measured for individual animals.

2.10 Biodistribution of DOX

When the average volume of the tumors reached 150 mm^3 in mice bearing LLC tumors, ZOL solution was intravenously administered *via* lateral tail veins at a dose of 40 μg of ZOL/mouse on days 0, 1 and 2, and then Doxil® was intravenously administered at a dose of 5 mg of DOX/kg on day 3. The tumors and organs were excised 24 h after the injection of Doxil®, and then homogenized in 0.1 M NH_4Cl/NH_3 buffer (pH 9.0). DOX was extracted with chloroform/methanol (2:1 v/v) and analyzed by high performance liquid chromatography (HPLC), as previously described.[55)]

2.11 Statistical analysis

The statistical significance of differences between mean values was determined by Student's t-test. Multiple measurement comparisons were performed by analysis of variance followed by one-way analysis of variance on ranks with post hoc Tukey-Kramer's test. A *p* value of 0.05 or less was considered significant.

III. RESULTS

3.1 Vascular structure of tumor after treatment with ZOL

Previously, it has been reported that the change of vascular structure in tumor was observed when ZOL solution was intravenously injected into mice bearing tumor;[57] however, the change of tumor environment upon ZOL treatments was not clear. In this study, ZOL treatment was investigated whether it could modulate the tumor environment *via* change of tumor vasculatures and enhance the antitumor efficacy of liposomal DOX, Doxil®.

First, to examine the frequency of ZOL administration and dosage amount (μg) of ZOL required to change the vascular structure in LLC tumor, ZOL solution was intravenously injected at a dose of 40 μg of ZOL/mouse per day for one, two or three consecutive days into mice bearing LLC tumor. When ZOL was injected for three consecutive days, apparent changes of vascular structure in the tumor were observed by immunostaining for CD31, which is a marker for endothelial cells, compared with those after one or two administrations (Fig. 5-A). Regarding dosage amount, changes of vascular structure in the tumor were observed upon ZOL injection at 5, 20 and 40 μg of ZOL/mouse per day for three consecutive days (Fig. 5-B). ZOL treatments reduced narrow vessels in tumor and increased open vessels, indicating that blood flow in tumor might be improved by the change of vasculatures structure. Furthermore, some CD31-positive endothelial cells were covered with α-SMA-positive pericytes in tumor section treated at 40 μg of ZOL/mouse for three consecutive days, although most of the CD31-positive endothelial cells in tumor section of untreated mouse were not covered with α-SMA-positive pericytes (Fig. 5-C), suggesting that ZOL treatments did not markedly affect pericyte coverage in tumor vessels. This histological change of tumor vasculatures after ZOL treatment seemed to be similar to the phenomenon called "normalization" of the tumor vasculatures.[9]

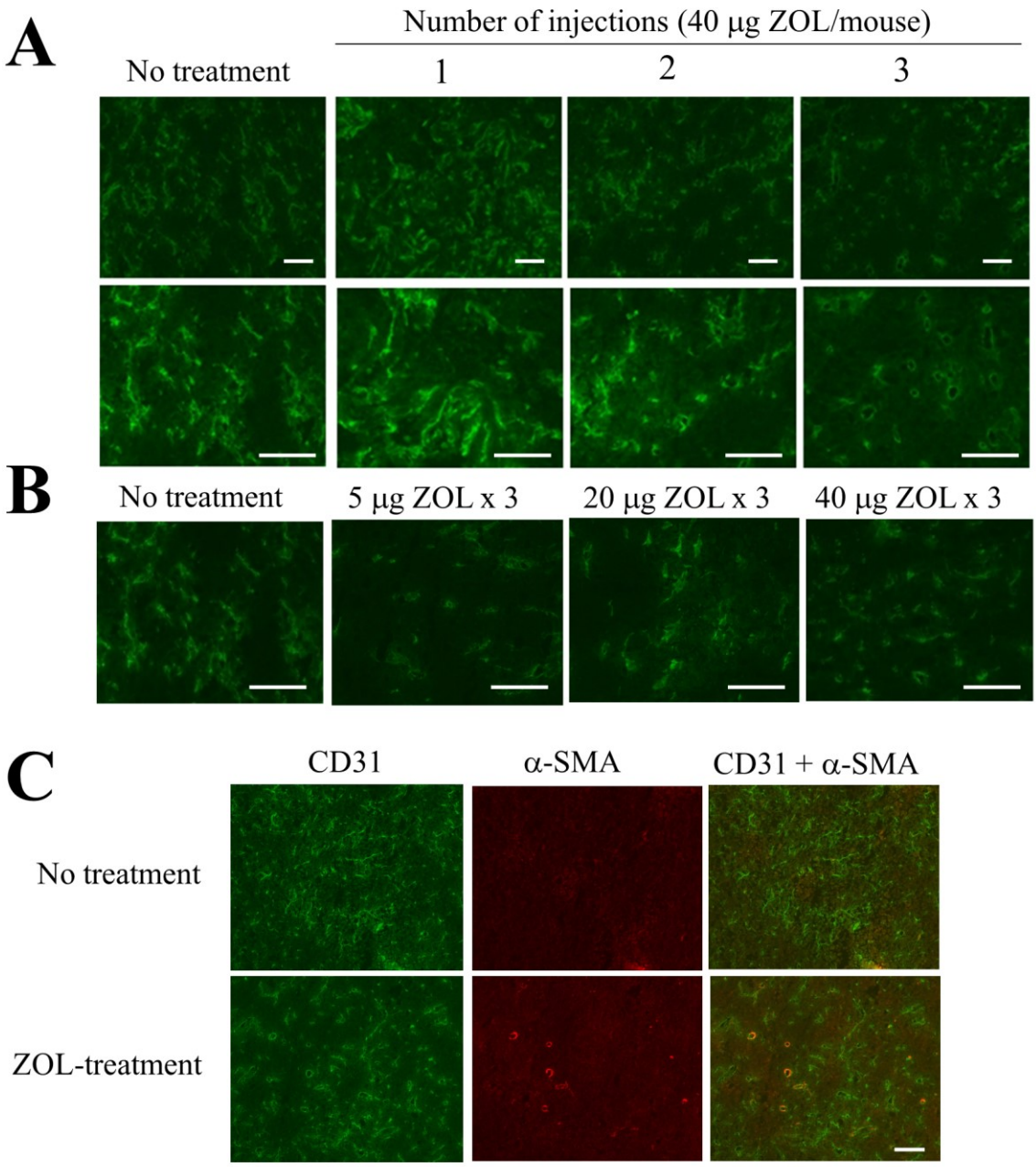

Figure 5. Immunostaining for endothelial cells after injection of ZOL into mice bearing LLC tumor. Green signals indicate CD31-positive endothelial cells. In A, ZOL solution was intravenously injected at a dose of 40 μg of ZOL/mouse per day into mice bearing tumor for one, two or three consecutive days. In B, ZOL solution was intravenously injected at a dose of 5, 20 or 40 μg of ZOL/mouse per day into mice bearing tumor for three consecutive days. In C, ZOL solution was intravenously injected at a dose of 40 μg of ZOL/mouse per day into mice bearing tumor for three consecutive days, and immunostaining for endothelial cells and pericytes was performed. Green signals indicate CD31-positive endothelial cells, and α-SMA-positive red signals indicate pericytes. Scale bar = 100 μm.

3.2 Change of IFP

To examine the effect of ZOL on IFP in tumors, IFP of tumors and muscles were measured at 24 h after intravenous injections of ZOL, and normalized the IFP of tumors by that of muscles. When ZOL solution was injected for three consecutive days, normalized IFP in LLC tumors was significantly decreased by injections of ZOL solution at 20 and 40 μg of ZOL/mouse per day (5.8 ± 1.3 and 5.9 ± 1.3 in normalized IFP, respectively) compared with that after injection of saline (9.1 ± 1.4 in normalized IFP), but not by 5 μg of ZOL/mouse per day (6.6 ± 2.6 in normalized IFP) (Fig. 6). This indicated that the injection of 20 or 40 μg of ZOL could decrease the IFP of the tumor by changing the tumor vasculatures. Therefore, in subsequent experiments, injections of 40 μg of ZOL/mouse per day were performed for three consecutive days.

It has been reported that Colon 26 and LLC tumors have well- and poorly vascularized blood vessels, respectively.[59] Compared to Colon 26, LLC tumors showed higher IFP.[58] When ZOL solution was injected into mice bearing Colon 26 tumor for three consecutive days, no decrease of IFP in the tumor was observed (2.4 ± 1.0 and 3.7 ± 1.2 of normalized IFP in Colon 26 tumor with no treatment and ZOL treatment, respectively) (data not shown). These findings suggest that reduction of IFP in tumor by ZOL treatments might be effective for tumors having high IFP.

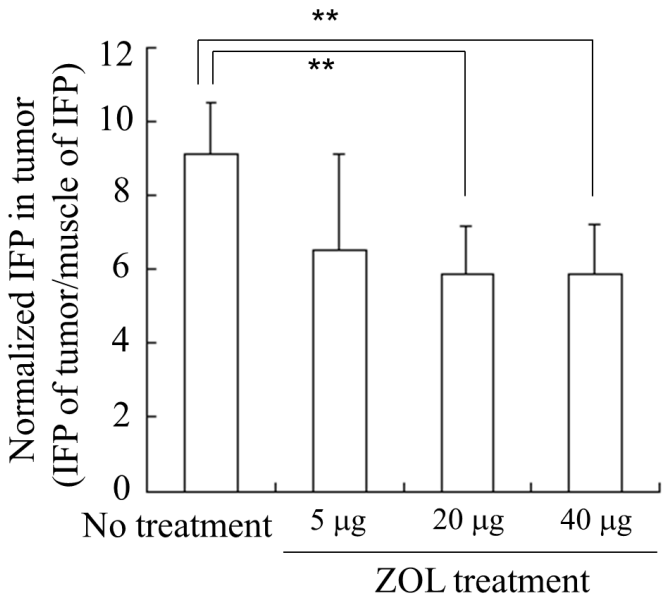

Figure 6. Change of IFP in LLC tumors after intravenous injection of ZOL. IFP in tumors was measured 24 h after intravenous injection of ZOL solution at a dose of 5, 20 or 40 μg of ZOL/mouse per day for three consecutive days into mice bearing tumors. Normalized IFP of tumors was calculated by dividing IFP of tumors (mmHg) by IFP of normal muscle (mmHg). Each column represents the mean ± S.D. (n=4-5). Statistical significance was evaluated by Student's *t*-test. $^{**}p<0.01$ compared with no treatment.

3.3 Change of macrophages in tumor and cytokine levels in serum after ZOL treatments

Bisphosphonates are internalized into cells by fluid-phase endocytosis, and then endosomal acidification causes the release of the bisphosphonates into the cytosol.[37] Highly phagocytic cells such as macrophages have the ability to internalize bisphosphonates, which makes them an ideal target for these drugs. Therefore, the effects of ZOL on macrophages were examined in tumor and liver. In untreated mice, a large number of macrophages in the livers and tumors was detected by immunostaining with F4/80 antibody; however, in ZOL treatments, the number of macrophages in the tumors and livers was markedly decreased (Fig. 7).

To examine the effect of ZOL treatments on the inflammatory cytokines in serum, IL-10, IL-12 (p70), GM-CSF and TNF-α level in serum were measured after ZOL treatment in mice with or without LLC tumor. The ZOL injections into mice without tumor decreased IL-12, GM-CSF and TNF-α levels compared with those in untreated mice without tumor, although their levels were not significantly different (Fig. 8-A). In contrast, the ZOL injections into mice bearing LLC tumor significantly increased IL-12 and TNF-α levels compared with those of untreated mice bearing LLC tumor. These findings suggest that ZOL injections may affect tumor cells or TAMs in tumor tissues and induce inflammatory responses.

The vascular endothelial growth factor (VEGF) protein is a prominent cytokine, which promotes endothelial cell proliferation during angiogenesis. Therefore, ZOL treatment was investigated for its effect on the expression level of VEGF mRNA in the tumor, by quantitative RT-PCR analysis. Surprisingly, VEGF mRNA level was not changed by ZOL treatments (Fig. 8-B), indicating that the change of vascular structure might be caused in an independent manner affecting VEGF expression.

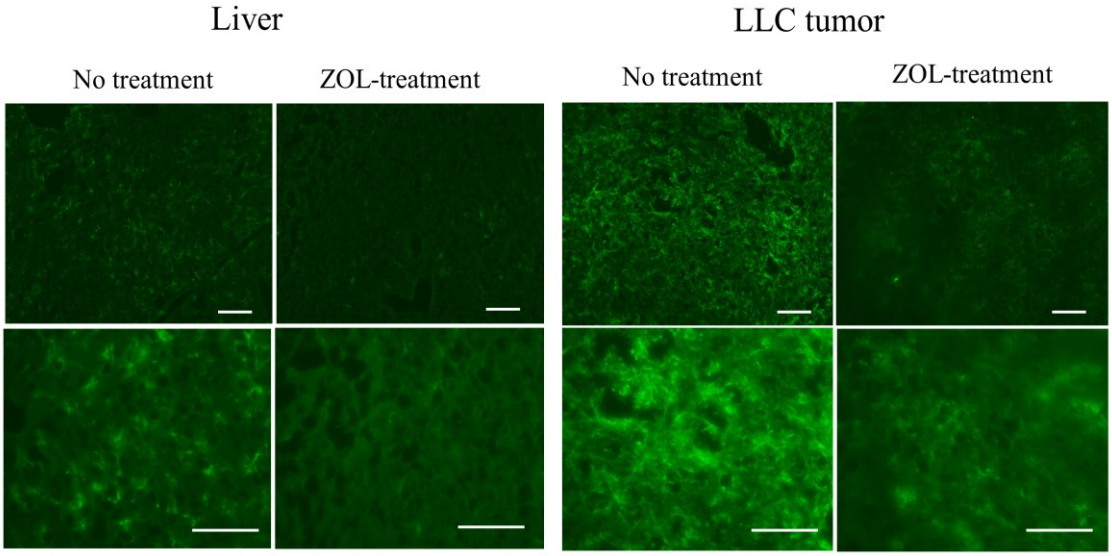

Figure 7. Immunostaining for macrophages in LLC tumor and liver after injection of ZOL into mice bearing LLC tumor. ZOL solution was intravenously injected into mice bearing tumor at a dose of 40 μg of ZOL/mouse per day for three consecutive days. Green signals indicate F4/80-positive macrophage cells. Scale bar = 100 μm.

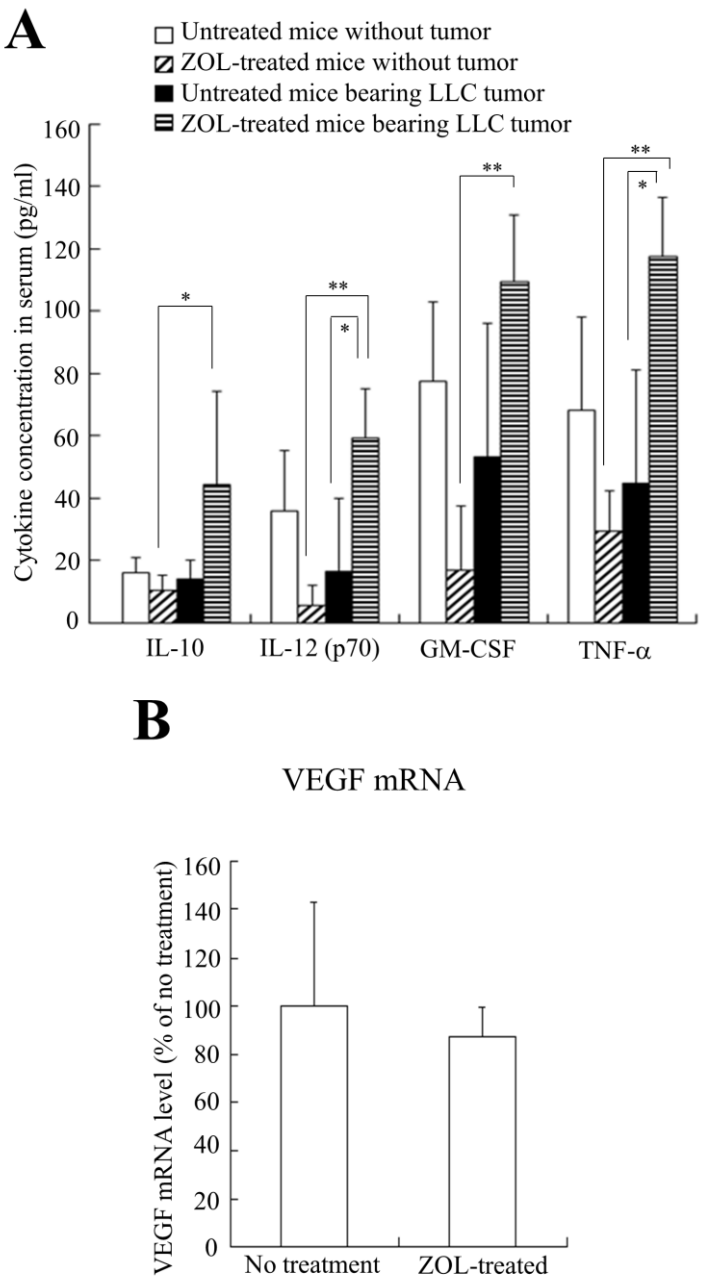

Figure 8. Cytokine levels in serum (A) and VEGF mRNA level (B) after ZOL injections. Mice with or without LLC tumor were intravenously injected with ZOL solution at a dose of 40 μg of ZOL/mouse per day for three consecutive days. In A, twenty-four hours after the final injection of ZOL solution, cytokine levels in the serum were determined. Each column represents the mean ± S.D. (n=3-4). The significance of differences between different groups was analyzed by one-way analysis of variance on ranks with post hoc Tukey-Kramer's test. $^{**}p<0.01$, $^{*}p<0.05$. In B, twenty-four hours after the final injection of ZOL solution, total RNA was purified from the tumors. Expression of mouse VEGF mRNA was analyzed by quantitative RT-PCR. Each result represents the mean ± S.D. (n=4).

3.4 *In vitro* antitumor effect

To confirm whether ZOL was taken up by tumor cells or macrophages and could induce cytotoxic effects, the cytotoxicity for LLC or RAW264.7 cells by ZOL were examined. ZOL treatment showed higher cytotoxicity for RAW264.7 cells than that for LLC cells (Fig. 9-A), indicating that this cytotoxicity by ZOL might be due to uptake by fluid-phase endocytosis in macrophage cells.

To examine the effect of ZOL on cytotoxicity by DOX, the cytotoxicities were examined for LLC or RAW264.7 cells by DOX in the presence of 20 μM ZOL. ZOL showed additive cytotoxic effects for RAW264.7 and LLC cells, rather than synergistic effects (Figs. 9-B,C), suggesting that ZOL could not increase chemo-sensitivity by DOX for macrophages or LLC tumors.

3.5 Antitumor effect on LLC tumor-bearing mice

To examine whether ZOL injections could increase the antitumor effect of Doxil® by change of the tumor microenvironment, the antitumor effect of Doxil® after three intravenous injections of ZOL was evaluated in LLC tumor-bearing mice. ZOL solution was intravenously administered on days 0, 1 and 2, and then Doxil® was on day 3. Three injections of ZOL solution did not show antitumor activity for the tumors (Fig. 10-A), although they had an antiangiogenic effect (Fig. 5). Single injection of Doxil® showed a large antitumor effect. Furthermore, injections of ZOL could increase the antitumor activity by Doxil®. There were no remarkable differences in mouse body weight changes after the administration of ZOL and/or Doxil® (Fig. 10-B).

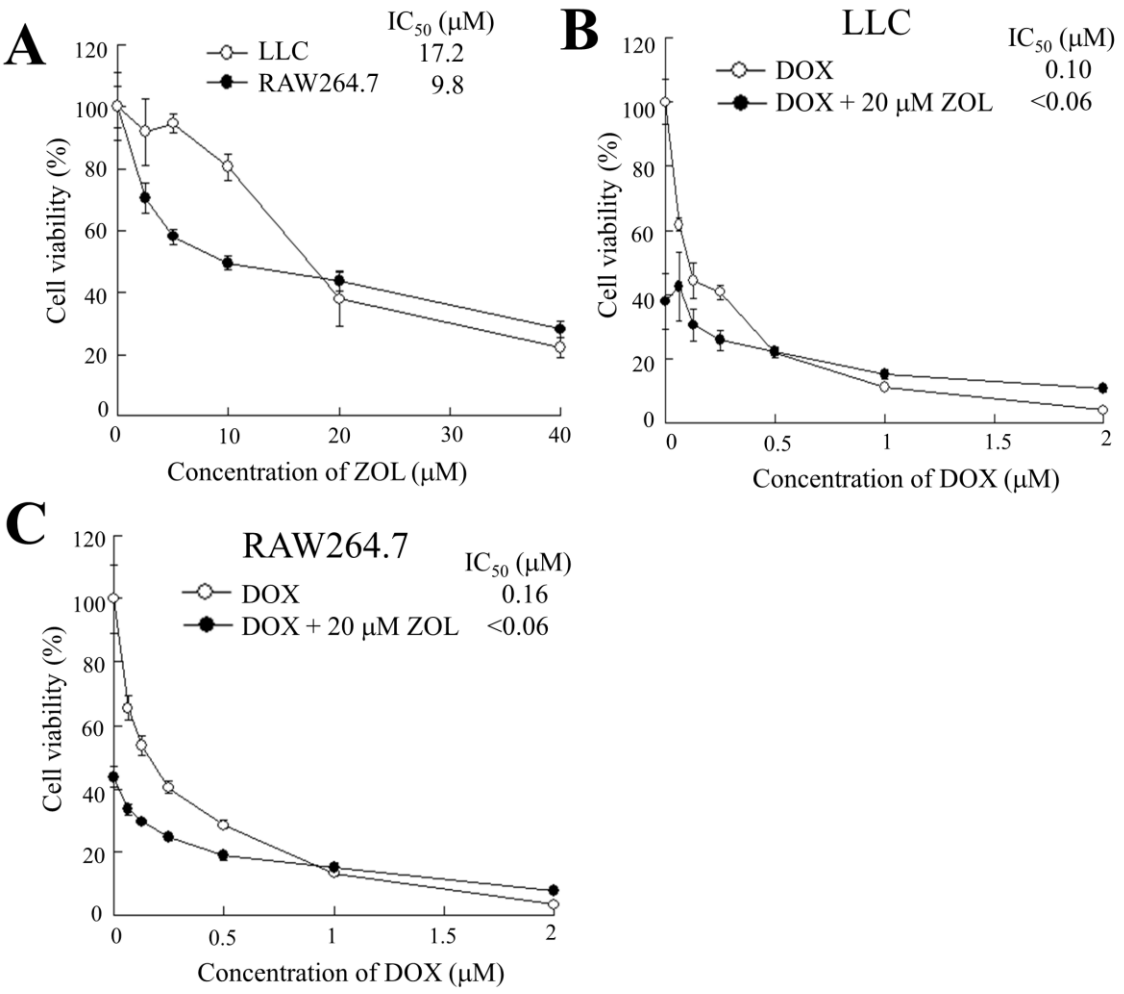

Figure 9. Cytotoxicities of ZOL for LLC and RAW264.7 cells (A) and of the combination of ZOL plus DOX for LLC (B) and RAW264.7 cells (C). In A, LLC and RAW264.7 cells were treated with various concentrations of ZOL for 48 h. In B and C, LLC (B) and RAW264.7 cells (C) were treated with various concentrations of DOX in the presence or absence of 20 μM ZOL for 48 h. Each result represents the mean ±S.D. (n=4).

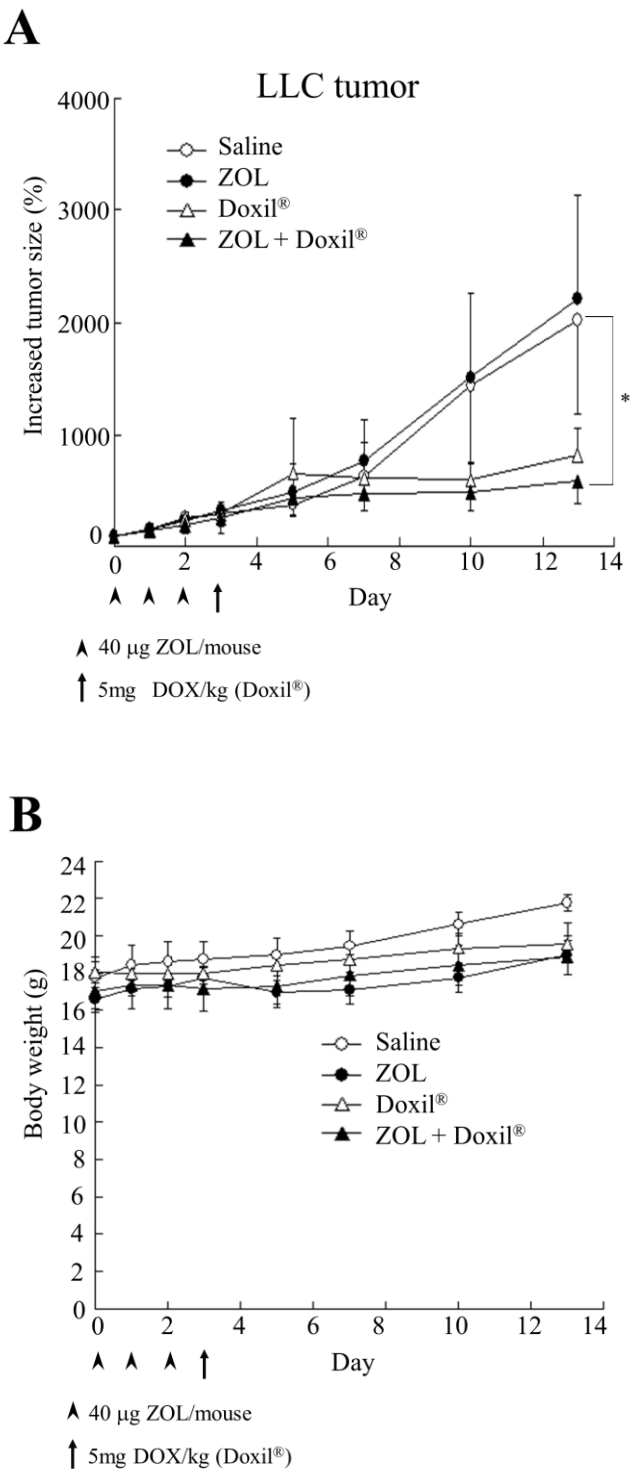

Figure 10. Combination therapy of ZOL and Doxil® in mice bearing LLC tumor. Antitumor activity and toxicity were assessed by measuring tumor volume (A) and body weight change (B). Saline (○), ZOL solution (●), Doxil®(△) and ZOL solution plus Doxil® (▲) were administered on days 0, 1 and 2 for ZOL injection and on day 3 for Doxil®. Arrow heads indicate the day of ZOL injection, and the arrow shows the day of Doxil® injection. Each value represents the mean ± S.D. (n = 3-4). The significance of differences between different groups was analyzed by one-way analysis of variance on ranks with posthoc Tukey-Kramer's test.*p<0.05.

3.6 Accumulation of DOX liposomes in tumor

Finally, whether ZOL treatments affected the biodistribution of DOX was examined in mice bearing LLC tumors after the injection of Doxil®. ZOL injections significantly increased the blood concentration of DOX after the injection of Doxil®, and decreased the accumulation of DOX in the liver (Fig. 11). The change of DOX accumulation in the liver may have been due to the depletion of Kupffer cells. However, the accumulation of DOX in the tumor was not significantly different between untreated and ZOL-treated tumors. These findings indicate that an increase of the antitumor effect of Doxil® upon ZOL injections might be explained by an increased blood circulation time of Doxil® and/or wide distribution of DOX in the tumor by a change of the tumor microenvironment.

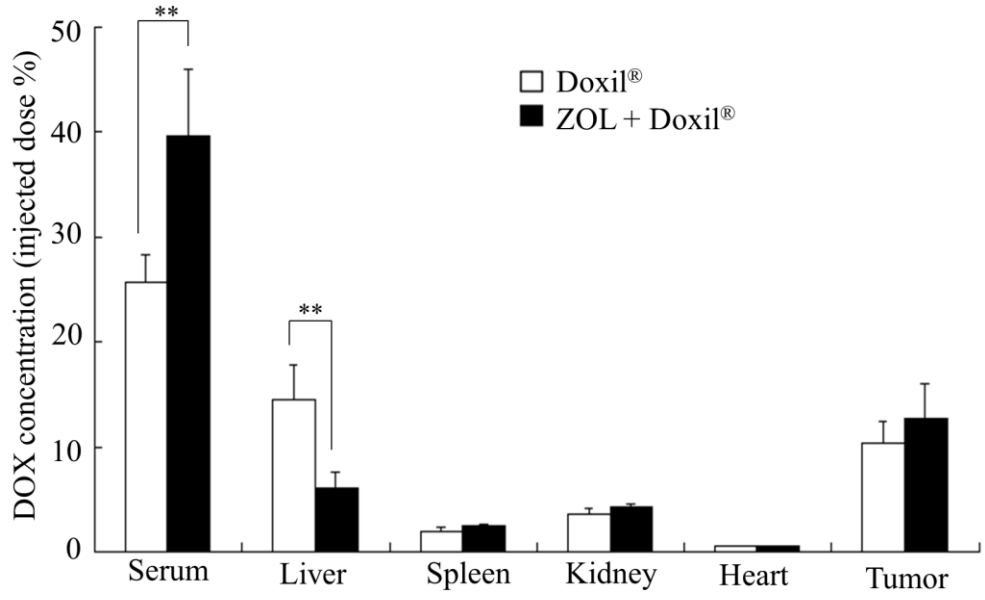

Figure 11. Effect of ZOL on the biodistribution of DOX at 24 h after the intravenous administration of Doxil® into mice bearing LLC tumor. ZOL solution was intravenously injected into mice bearing tumor at a dose of 40 μg of ZOL/mouse per day for three consecutive days. Twenty-four hours after the final injection of ZOL solution, Doxil® was intravenously injected at 5 mg of DOX/kg. DOX concentrations in serum, liver, spleen, kidney, heart and tumor were measured at 24 h after the injection of Doxil® by HPLC. Each value represents the mean ± S.D. (n = 3-4). Statistical significance was evaluated by Student's *t*-test. ** $p<0.01$.

IV. DISCUSSION

Antiangiogenesis effects are known to change the tumor vasculatures. In this study, ZOL treatment has been found to decrease IFP in tumor *via* the inhibition of tumor neovascularization (Figs. 5 and 6). Santini et al. reported that single treatment of ZOL reduced circulating VEGF levels in cancer patients.[60] However, in this study, a reduction of VEGF mRNA was not observed in tumors after ZOL treatments (Fig. 8-B). Ogawara et al. reported that VEGF did not play a major role in the angiogenesis in LLC tumor, suggesting that other proangiogenic factors except for VEGF might trigger angiogenesis in LLC tumor.[59] Giraudo et al. reported that ZOL suppressed the expression of matrix metalloproteinase-9 (MMP-9) by infiltrating macrophages and inhibited metalloproteinase activity, reducing the association of VEGF with its receptor on angiogenic endothelial cells.[61] From these findings, the depletion of TAMs in tumor by ZOL treatments might affect tumor neovascularization *via* inhibition of the association of VEGF and its receptor. However, it has also been reported that ZOL inhibited antiangiogenesis through an apoptotic effect on endothelial cells in tumor and the tumor microenvironment.[62,63] ZOL exerts an inhibitory effect on endothelial cell adhesion and migration *via* the modulation of adhesion molecules.[64] The mechanism by which ZOL treatments changed the vascular structures in the tumors was not clear, but ZOL treatments could decrease IFP in tumor *via* the inhibition of tumor neovascularization.

The most common adverse event associated with bisphosphonate therapy is transient fever.[65] It has been shown that treatment with intravenous nitrogen-containing bisphosphonates such as ZOL caused systemic acute-phase responses (APRs) characterized by fever, pain, nausea and fatigue in up to 50% of all patients within 48 hours after administration.[66] These flu-like symptoms are typically transient, resolve spontaneously, and are accompanied by decreased lymphocyte counts and elevated levels of pro-inflammatory

cytokines such as IL-6, IFN-γ and TNF-α.[67,68] In this study, elevated levels of IL-10 and -12, GM-CSF and TNF-α were observed after injections of ZOL solution into mice bearing tumor (Fig. 8-A); however, in normal mice without tumor, ZOL injections did not affect the level of inflammatory cytokines in serum. Although it was not clear why the ZOL treatments increased the levels of the inflammatory cytokines in mice bearing tumor, these cytokines might be released from tumor tissues by ZOL treatments and cause inhibition of tumor neovascularization.

Polyethylene glycol (PEG)-modified liposomes are long-lived in the circulation and accumulate passively in tumors. The TGF-β type I receptor inhibitors were reported to increase the antitumor effect of DOX encapsulated in PEGylated liposomes or micelles by changing the microenvironment of the vasculatures.[54,55] Therefore, whether ZOL treatments could increase the accumulation of Doxil® in tumor and enhance the antitumor effect were examined. In terms of the results, ZOL treatments could increase the antitumor effect of Doxil® (Fig. 10); however, they could not increase the accumulation of DOX in the tumor 24 h after the injection of Doxil® (Fig. 11). ZOL is known as a specific inhibitor of farnesyl pyrophosphate synthase in the mevalonate pathway and exerts pleiotropic effects in tumor and non-tumor cells.[68,69] Riganti et al. reported that ZOL restored the chemosensitivity of DOX in multidrug-resistant cancer cells.[70] However, in this study, ZOL treatments alone did not induce an antitumor effect for LLC tumor (Fig. 10), and did not show enhancement of cytotoxicity by DOX in LLC cells (Fig. 9-B). Yoshizawa et al. reported that pre-treatment with a VEGF receptor-2 inhibitor, SU5416, changed vascular structures in tumor but did not significantly increase the tumor accumulation of paclitaxel after the injection of PEGylated liposomal paclitaxel, compared with the case in untreated mice.[71] However, they concluded that the treatment increased the distribution of PEGylated liposomal paclitaxel in the core region of the tumor, as well as conversely decreasing the ratio of its peripheral distribution.

Therefore, the enhanced antitumor effect observed in an *in vivo* experiment might be due to the improvement of DOX distribution in tumor, not an increase of DOX chemosensitivity in tumor cells, speculatively. To prove this hypothesis, the localizations of DOX was observed in tumor after ZOL treatments by fluorescent microscopy, but the localization was not well detected due to the weak intensity of DOX fluorescence (data not shown). Further study should be performed to investigate the distribution of DOX in tumor after ZOL treatments.

Resident macrophages in the liver called Kupffer cells comprise the major population of the reticuloendothelial system (RES). Doxil® can avoid RES uptake by PEG modification; however, the effectiveness for the prevention of RES uptake is still incomplete. Previously, it was reported that the depletion of Kupffer cells by clodronic acid-entrapped liposomes (clodrolip) inhibited RES uptake in the liver and increased the plasma concentration of DOX after the injection of Doxil®, resulting in enhancement of antitumor effects in a xenograft model.[72)] In this study, depletion of Kupffer cells (macrophages) in the liver was observed after the injection of ZOL (Fig. 7), and exhibited extended blood circulation of DOX and reduced its accumulation in the liver (Fig. 11). This depletion might be one of the reasons why the combination of ZOL and Doxil® could enhance therapeutic efficacy.

Ottewell et al. reported that the inhibition of tumor growth was observed by sequential injection with DOX and ZOL in a mouse model of breast and mammary tumor.[38,73)] They concluded that sequential treatment with DOX followed by ZOL could elicit substantial antitumor effects *in vivo*, but ZOL followed by DOX could not.[38)] The discrepancy between the present works and previous reports might be caused by the schedule of administration of ZOL and DOX. In sequential treatment with ZOL followed by DOX, DOX was injected into the mice 24 h after the injection of ZOL; however, the tumors after ZOL treatment displayed no obvious differences in terms of the degree of vascularization compared with the saline control.[38)] In this experiment, no change of vascular structure in LLC tumors was observed 24

h after single injection of ZOL (Fig. 5-A). These results might indicate that the repeated injections of ZOL were needed to increase the antitumor effect by the change of vascular structures.

In this study, it has been observed that ZOL treatments could decrease IFP in tumor *via* a change of tumor vasculatures and enhance the antitumor efficacy of liposomal DOX (Doxil®), thus suggesting that ZOL treatment can be an alternative approach to increase the antitumor effect by liposomal drug.

Chapter 2

Tumor delivery of liposomal doxorubicin prepared with poly-L-glutamic acid as a drug-trapping agent

1. INTRODUCTION

The high and stable drug loading into liposomes has become a critical factor for successful delivery of DOX to tumor since nanosized liposomes can passively accumulate in solid tumors *via* the EPR effect.[41)] However, modification of drug release from liposome should be considered to increase the antitumor activity in tumor tissue. DOX, which is a weak amphipathic base, exists as stable bundles of fiber-like aggregates in the liposomal interior as the result of over drug solubility limits and its interaction with sulfate ions during ammonium gradient-driven drug loading, as observed in DOXIL®.[41,45)] These DOX aggregates showed high drug retention during circulation in the bloodstream, which led to an enhanced antitumor efficacy *via* the EPR effect.[41,74–76)] However, it has been reported that only small amount of biologically active DOX was observed in nucleus after DOXIL® is taken up by cells.[42)] The intrinsic stability of DOXIL® prevents DOX released from liposome intracellularly. Therefore, it is important to select drug trapping agents appropriately to improve tumor delivery and efficacy of DOX.

It has been reported that the physical state of drug entrapped in liposomes affects drug retention.[48)] The use of anionic trapping agents such as polyphosphates and highly charged anionic sucrose octasulfate has been reported to improve anticancer activity of weak base drug, i.e. irinotecan.[47,77)] These trapping agents increased the intraliposomal retention of irinotecan, resulted in reduced drug release and prolonged circulation of drug associated with trapping agents in liposome.

PGA is an anionic polymer that can be ionized and interact with cationic amines of DOX. It is also biodegradable with non-toxic degradation products.[78–80)] Therefore, the use of PGA as an intraliposomal drug trapping agent may provide benefits for tumor delivery of liposomal DOX. It has been reported that the ionic interaction between poly-γ-glutamic acid

and DOX produced random colloidal aggregates that were stable in pH 7.4, but showed high release in lower pH, provided a pH-controlled release.[51] The low pH of endosomal compartment has been known as a useful target for pH-dependent drug release from liposomes,[81] where DOX should be released and intercalates with DNA in nucleus right after liposome is taken up by endocytosis to achieve its antitumor effect, or it will be degraded in lysosomes and becomes ineffective.[42]

In this chapter, the PGA was investigated as an internal trapping agent for stable liposomal encapsulation of DOX loaded *via* triethylamine (TEA) gradient. The effects of concentration or molecular weight of PGA in TEA-PGA liposomes were evaluated on the accumulation of DOX in tumors and their antitumor effects in LLC tumor-bearing mice.

II. MATERIALS AND METHODS

2.1 Materials

Hydrogenated soya phosphatidylcholine (HSPC) and methoxy-(polyethylene-glycol)-distearylphosphatidyl-ethanolamine (mPEG-DSPE, PEG mean molecular weight, 2000) were purchased from NOF Inc. (Tokyo, Japan). Cholesterol (Chol), ammonium sulfate (AS) and triethylamine (TEA) were purchased from Wako Pure Chemical Industries Inc. (Osaka, Japan). DOX hydrochloride was obtained from LC Laboratories (Woburn, Massachusetts, USA). PGA sodium salt was purchased from Sigma (Tokyo, Japan) and has three types with mean molecular weight of 4800, 9800, and 20500. All other chemicals and solvents used in this study were of the highest grade available.

2.2 Preparation of liposomes

TEA-PGA-Ls, TEA liposomes (TEA-L), and AS liposomes (AS-L) were prepared with HSPC, Chol, and mPEG-DSPE at a molar ratio of 4.1:2.7:0.4 using the thin-film method.[82)] Firstly, all the lipids were dissolved in chloroform and placed in a round bottom flask. The thin films formed following the removal of chloroform using a rotary vacuum evaporator in a water bath at 60˚C. In AS-L and TEA-L, lipids were hydrated with 0.25 M AS solution and 0.65 M TEA solution, respectively. In TEA-PGA-Ls, lipids were hydrated with 0.65 M TEA solution containing PGA, as shown in Table 1. After hydration, the lipids were vortexed to prepare liposomes, followed by heating in a water bath at 60˚C for 5 min. The liposomes were sonicated for 30–60 min to produce a final size about 100 nm. For replacement of the external phase, liposomes were passed through a gel filtration column (Sephadex G100) with phosphate-buffered saline (PBS, pH 7.4). The loading of DOX was then performed by incubating liposomes with DOX solution at weight ratio of DOX:HSPC of

1:5 in a water bath at 60˚C for 10 min. Free DOX was separated from AS-L, TEA-L, and TEA-PGA-Ls through a column packed with Sephadex G50. The concentration of phospholipids was quantified using a Phospholipid C-test reagent (Wako Pure Chemical Industries, Ltd.). The entrapped DOX concentration was measured using a fluorometric method at λ_{ex}= 485 nm and λ_{em}= 590 nm after lysing with Triton X-100 (final concentration 5% v/v). Drug loading was calculated as follows:

$$Percent\ of DOX\ loading = \frac{\text{amount of DOX entrapped inside liposome}}{\text{total amount of DOX}} \times 100\%$$

2.3 Measurement of particle size and ζ-potential of liposomes

The average particle size and ζ-potential of the liposomes were measured by a cumulative method and electrophoretic mobility with a light scattering photometer (ELS-Z2, Otsuka Electronics Co., Ltd., Osaka, Japan) at 25˚C after dilution in an appropriate volume of deionized water.

2.4 Evaluation of DOX/PGA complex formation

By assuming that liposomes with diameter of 120 nm contained about 4.8 μL of total entrapped vesicular volume per 1 mg of liposomal lipids, we could estimate the ratios of DOX and PGA inside liposomes, as shown in Table 1. A mole of PGA was calculated as L-glutamic acid monosodium salt. To evaluate complex formation, the DOX solution was mixed with PGA solution in 0.65 M TEA at the indicated ratios and then left at room temperature for at least 30 min. As a control, DOX solution was mixed with 0.25 M AS solution, L-glutamic acid solution, and 0.65 M TEA solution, respectively. Photomicrographs of the mixtures were taken using an optical microscope (Nikon Eclipse TS100-F, Nikon Inc., Japan).

2.5 Small angle X-ray diffraction (SAXRD) analysis of liposomal DOX

The small angle X-ray diffraction (SAXRD) analysis of liposomal DOX was evaluated using the facility on the BL-6A beam line at the National Laboratory for High Energy Physics (KEK, Tsukuba, Japan). The experimental hutch in BL-6A is equipped with a marble table housing the modular-length flight tube and 2D detector (Pilatus3 1M). The liposomes were loaded into a 1.8 mm diameter quartz capillary cell using a peristaltic pump, and were set to be put within a 50 cm range of the detector. Data were collected by measuring at an energy of 8.27 keV with an exposure time of 20 s per frame at an X-ray wavelength of 1.5 Å using the dedicated beam line software PILATUS Measurement Control Software at Photon Factory. Data processing, and further analysis were performed using ATSAS software (https://www.embl-hamburg.de/biosaxs/primus.html, Hamburg, Germany).[83)]

2.6 *In vitro* doxorubicin release from DOX/PGA aggregate and liposomal DOX

DOX/PGA aggregate was prepared by mixing DOX with PGA_{20500} at molar ratio of DOX/PGA of 5.8 in 0.65 M TEA solution. One mole of PGA was calculated based on L-glutamic acid monosodium salt. As a model of aggregate entrapped in AS-L, DOX/AS aggregates were prepared by mixing DOX in 0.25 M AS. The aggregates were left at room temperature for 30 min after mixing. The study of DOX release from DOX/PGA or DOX/AS aggregates was performed by placing 200 μL of aggregate suspension in dialysis tubing Spectra Por®7 with molecular weight cut-off (MWCO) 3,500 (Spectrum Laboratories, Inc., Rancho Dominguez, CA, USA). The dialysis tubing was immersed in a 50 mL of PBS pH 5.5 or 7.4 with continuous stirring in a water bath at 37˚C.

The release studies of DOX from liposomes were performed by placing 200 μL of liposome solution into dialysis tubing Spectra Por®7 with MWCO 3,500 (Spectrum

Laboratories, Inc.). The liposomes were then immersed in 50 mL of PBS, pH 7.4, with continuous stirring in a water bath at 37˚C.

At various time points, 200 μL aliquots were withdrawn from the outer aqueous solution and replaced by 200 μL of PBS. The DOX concentration was measured fluorometrically at λ_{ex}= 485 nm and λ_{em}= 590 nm. Wurster correction was used for calculating the cumulative amount of DOX released.

2.7 *In vitro* cytotoxic assay of liposomes

Murine LLC cells were obtained from the Cell Resource Center for Biomedical Research, Tohoku University (Miyagi, Japan). LLC cells were cultured in RPMI-1640 medium with 10% heat-inactivated fetal bovine serum and kanamycin (100 μg/ml) in a humidified atmosphere containing 5% CO_2 at 37˚C. For the *in vitro* cytotoxic assay, LLC cells were seeded separately at a density of 1×10^4 cells per well in 96-well plates and maintained in the medium for 24 h before treatment.

To examine the cytotoxicity for DOX, the cells were treated with medium containing various concentrations of DOX in AS-L, TEA-L, or TEA-PGA-Ls, and they were then incubated for 48 h. After treatment, the cell number was determined using Cell Counting Kit-8 (Dojindo Laboratories, Kumamoto, Japan). Cell viability was expressed relative to absorbance at 450 nm in untreated cells, and the concentration leading to 50% cell viability (IC_{50}) was calculated.

2.8 Antitumor activity of liposomal DOX

All animal experiments were performed with approval from the Institutional Animal Care and Use Committee of Hoshi University. To generate LLC tumors, 1×10^6 cells suspended in 100 μL PBS, pH 7.4 were inoculated subcutaneously into the right flank of

female C57BL/6N mice (7 weeks old, Sankyo Labo Service Corp.). After the tumor size had reached about 100–200 mm^3, AS-L, TEA-L, and TEA-PGA-Ls were administered *via* the tail vain at doses equal to 5 mg DOX per kg mouse by single-dose injection on day 0. Tumor volume and body weights were measured for individual animals. The tumor volume was calculated using the following formula: tumor volume = $0.5 \times a \times b^2$, where a and b are the larger and smaller diameters, respectively.

2.9 Biodistribution of liposomal DOX

To generate LLC tumors, 1×10^6 cells were inoculated subcutaneously into the flank of female C57BL/6N mice (female, 7 weeks old). After the tumor size had reached 200 mm^3, AS-L, TEA-L, and TEA-PGA-Ls were administered intravenously *via* the tail vein at a dose equivalent to 5 mg DOX per kg. Twenty-four hours after injection, blood was collected from the inferior vena cava and centrifuged to obtain serum. The tumor, liver, spleen, kidney, lung, and heart were excised and homogenized in 0.1 M NH_4Cl/NH_3 buffer and DOX was extracted with chloroform-methanol (2:1 v/v). The DOX concentration was further quantified using HPLC method as previously described.[55)]

2.10 Statistical analysis

All data were produced in replicates and presented as the mean ± S.D. To evaluate the significance of the difference, data were analyzed by one-way ANOVA, followed by Tukey's HSD post-hoc test; *P* values less than 0.05 were considered as statistically significant.

III. RESULTS

3.1 Preparation and characterization of liposomal DOX using PGA

To evaluate the effect of PGA as a liposomal trapping agent, the PGA-TEA system was used to prepare liposomal DOX. TEA can assist in the loading of weakly basic-amphipathic drugs *via* TEA efflux, accompanying the influx of the drug into liposomes and through the formation of self-perpetuating pH gradient providing a driving force for drug accumulation.[47,84)] These mechanisms may be able to maintain DOX in ionized forms and then increase intraliposomal stability by electrostatic interactions between DOX and PGA.

TEA-PGA-Ls were prepared by remote loading of DOX with a TEA gradient into pre-formed liposomes prepared with 1, 2, or 4 mg/mL PGA (molecular weights 4800, 9800, or 20500) (Table 1). However, in TEA-PGA_{20500}-L, it was difficult to obtain small, homogenous liposomes prepared with 4 mg/mL PGA_{20500} because of its high viscosity. Moreover, in the preliminary study, we evaluated the effect of incubation time and drug-to-lipid ratio on the entrapment of DOX in TEA-PGA-L. In TEA-L and TEA-PGA_{9800}-C2-L, with only 10 min incubation at 60˚C, most DOX could be entrapped into liposomes, and extending the incubation period for 30 or 60 min decreased entrapment efficiency of DOX (data not shown). Furthermore, the highest entrapment efficiency was observed in liposomes prepared at a DOX:HSPC ratio of 1:5 (w/w) compared with 1:2 or 1:1 (data not shown). From these results, a 10-min incubation at 60˚C and DOX-to-HSPC ratio of 1:5 (w/w) were chosen for loading of DOX.

As shown in Table 1, all the liposomes had average particle sizes around 110 nm, with negative charges of particles equivalent to approximately -15 mV. All the TEA-PGA-Ls showed high entrapment efficiency of DOX (>95%) similar to liposomes using ammonium

sulfate (AS-L) and TEA (TEA-L). The molecular weight and concentration of PGA in TEA-PGA-Ls did not affect the particle size, ζ-potential, or entrapment efficiency of DOX.

3.2 Evaluation of DOX-PGA complex formation

To evaluate the interaction of PGA with DOX, we mixed DOX solution with PGA and then observed the mixture by microscopy. To estimate the intraliposomal conditions, the molar ratio of PGA and DOX inside the liposomes was calculated based on the concentration of DOX and total vesicular volume. When PGA and DOX were mixed at estimated molar ratios of DOX/PGA as listed in Table 1, aggregate-like substances were observed (Figs. 12-A-E), which had different structures compared with aggregates formed by mixing of DOX and AS solution (Fig. 12-F). Furthermore, an increase in molecular weight or concentration of PGA in the mixture of PGA and DOX resulted in larger aggregates. On the other hand, no aggregates were observed with the mixture of DOX and L-glutamic acid (Fig. 12-G) or DOX in TEA solution (Fig. 12-H). These results indicated that PGA might electrostatically interact with DOX inside liposomes and facilitate the encapsulation of DOX in TEA-PGA-Ls.

Table 1. Composition and characteristics of liposomal DOX.

Formulation	Hydrating solution	Estimated mole ratio of DOX/glutamic acid in liposomes[a)]	Particle size (nm)[b)]	ζ-Potential (mV)[b)]	Entrapment efficiency (%)[b)]
AS-L	0.25 M ammonium sulfate (AS)	-	109.4 ± 7.8	-19.4 ± 8.0	97.9 ± 1.1
TEA-L	0.65 M triethylamine (TEA, pH 6.7)	-	118.9 ± 8.2	-13.9 ± 5.6	97.6 ± 1.2
TEA-PGA_{4800}-C2-L	2 mg/mL PGA_{4800} in 0.65 M TEA	5.8	112.5 ± 3.6	-13.5 ± 2.4	95.1 ± 0.8
TEA-PGA_{9800}-C1-L	1 mg/mL PGA_{9800} in 0.65 M TEA	11.7	110.7 ± 1.5	-11.9 ± 5.5	98.1 ± 1.5
TEA-PGA_{9800}-C2-L	2 mg/mL PGA_{9800} in 0.65 M TEA	5.8	112.5 ± 8.9	-12.9 ± 1.9	98.2 ± 1.9
TEA-PGA_{9800}-C4-L	4 mg/mL PGA_{9800} in 0.65 M TEA	2.9	110.8 ± 2.4	-15.6 ± 5.5	95.0 ± 6.3
TEA-PGA_{20500}-C2-L	2 mg/mL PGA_{20500} in 0.65 M TEA	5.8	118.5 ± 10.3	-12.1 ± 4.3	97.4 ± 4.6

[a)] PGA mole was converted to L-glutamic acid monosodium salt unit.

[b)] Each value represents the mean±S.D. (n=3).

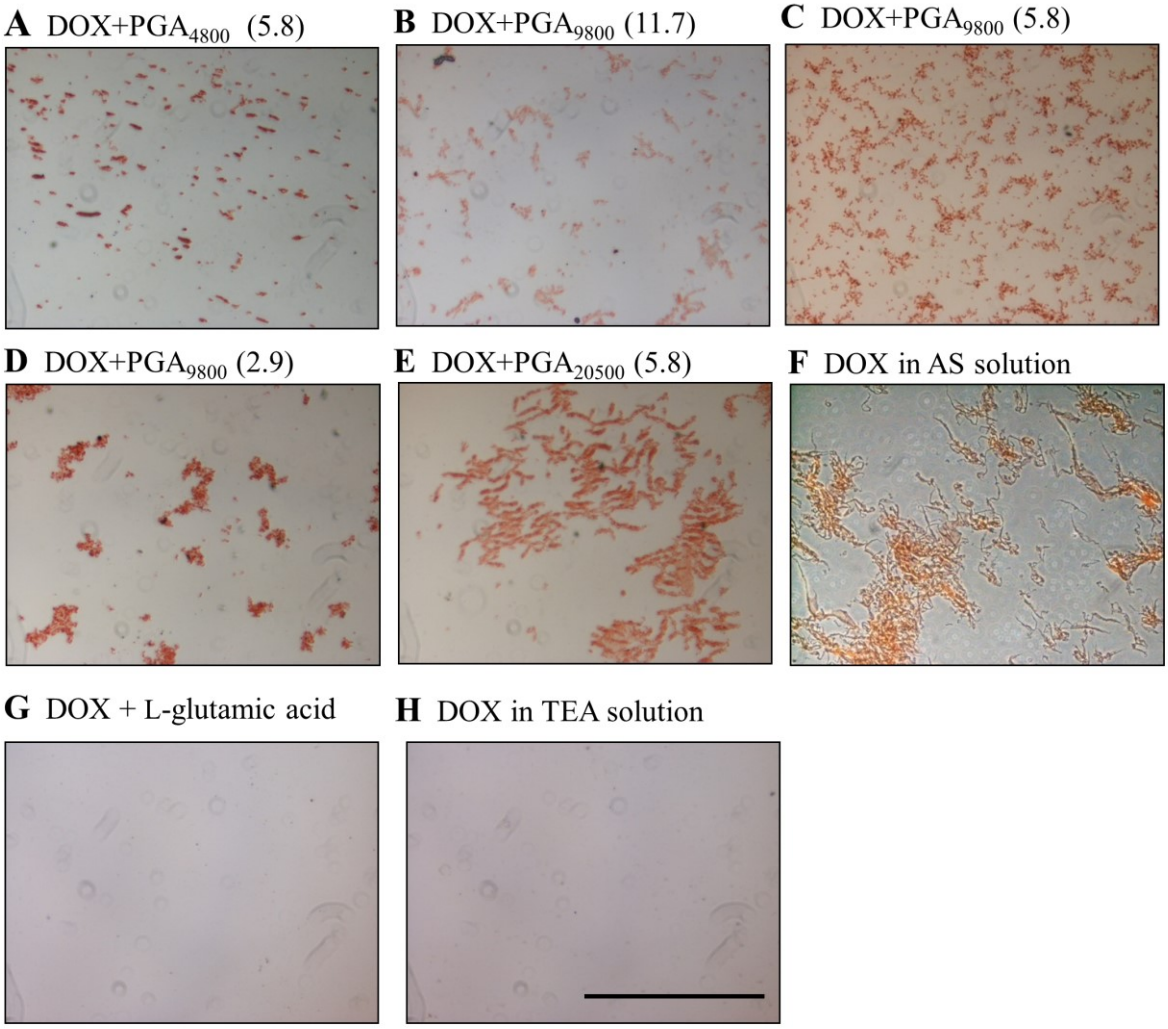

Figure 12. Microscopic observation of mixtures of DOX and PGA (A-E), DOX in 0.25 M ammonium sulfate (AS) solution (F), mixture of DOX and L-glutamic acid solution (DOX/ L-glutamic acid at molar ratio of 5) (G), and DOX in 0.65 M triethylamine (TEA) solution (H). The number in parentheses represents the estimated molar ratio of DOX and PGA inside liposomes, as listed in Table 1. A mole of PGA was calculated as L-glutamic acid monosodium salt. Scale bar = 100 μm.

3.3 Small angle X-ray diffractions (SAXRD) analysis of liposomal DOX

To investigate the physical characteristics of their aggregates, small angle X-ray diffractions (SAXRD) of AS-L, TEA-L and TEA-PGA-Ls were measured after loading liposome with DOX at a weight ratio of DOX/HSPC of 1:5. As shown in Fig. 13, PGA-TEA-Ls and AS-L had almost identical patterns of scattering profile at scattering vector (q)

between 0.06 - 0.6 Å^{-1}. However, at q below 0.05 Å^{-1}, the difference of scattering intensities was observed between TEA-PGA-Ls and AS-L. In TEA-PGA-L, the addition of PGA into TEA-L increased the scattering intensity, indicated that TEA-PGA-Ls had DOX/PGA aggregates in the inner phase; however, the difference of scattering profiles of TEA-PGA$_{4800}$-C2-L and TEA-PGA$_{20500}$-C2-L was negligible (Fig. 13).

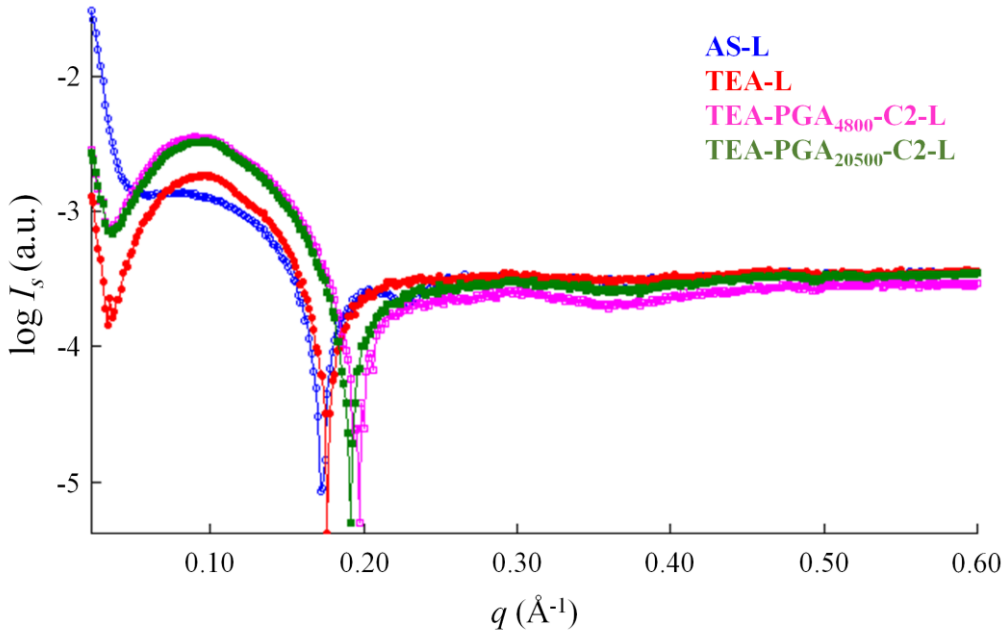

Figure 13. The profiles of small angle X-ray diffraction (SAXRD) of AS-L, TEA-L, and TEA-PGA-Ls prepared at a DOX:HSPC weight ratio of 1:5. Data are plotted as scattering intensity (I_S) in arbitrary units as a function of the scattering vector (q) in Å^{-1}, where q is $4\pi\sin(\theta)/\lambda$.

3.4 Evaluation of *in vitro* DOX released from DOX-PGA aggregates

To examine the effect of the interaction between DOX and PGA inside liposomes, the amount of DOX released from DOX/PGA aggregates were determined in PBS at pH 5.5 or 7.4. Here, PGA with molecular weight of 20500 was used. In DOX/AS aggregates, regardless of pH, most of the DOX was released from the aggregate over 23 h (Fig. 14). In contrast, in PGA/DOX aggregates, the amount of DOX released at pH 7.4 was only 28% over 23 h. On

the other hand, at pH 5.5, the amount released was significantly increased twofold than that at pH 7.4 (Fig. 14). This finding suggested that PGA might have an advantage in the pH-sensitive release of DOX from PGA/DOX aggregates.

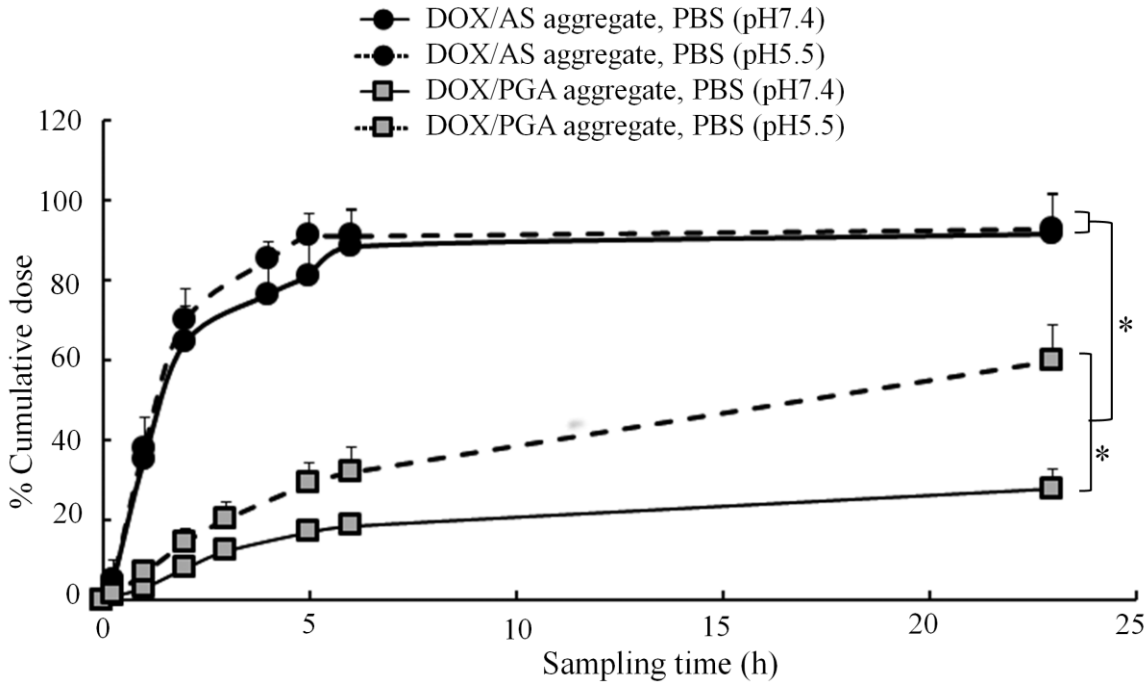

Figure 14. Profiles of DOX release from DOX/PGA and DOX/AS aggregates in PBS, pH 5.5 and 7.4. DOX/PGA_{20500} aggregates were prepared at a molar ratio of DOX/PGA of 5.8. A mole of PGA was calculated as L-glutamic acid monosodium salt. Each value represents the mean ± S.D. (n=3). *p< 0.05.

3.5 The effect of PGA on drug release from liposomes

The *in vitro* profiles of DOX release from liposomes were evaluated by immersing liposomes in PBS, pH 7.4 (Fig. 15). Compared with TEA-L, TEA-PGA-Ls showed reduced DOX release. Among the TEA-PGA-Ls prepared with 2 mg/mL PGA, TEA-PGA_{20500}-C2-L, which were prepared with the highest molecular weight PGA, showed the lowest release of DOX from liposomes of approximately 13% of the cumulative dose over 52 h, which was similar to AS-L. Furthermore, among TEA-PGA-Ls prepared at 1, 2, and 4 mg/mL PGA_{9800}, the TEA-PGA_{9800}-C4-L, which was prepared with 4 mg/mL PGA_{9800}, yielded slower release

of DOX than TEA-PGA$_{9800}$-C1-L and TEA-PGA$_{9800}$-C2-L that were prepared with 1 and 2 mg/mL PGA$_{9800}$, respectively.

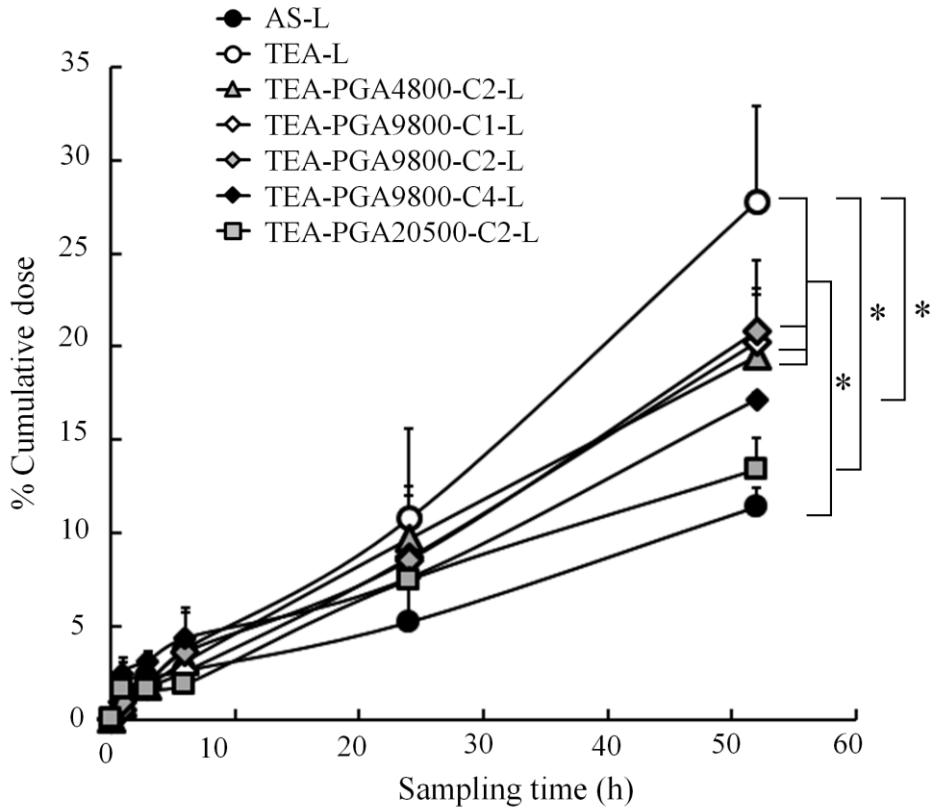

Figure 15. Profiles of release of DOX from TEA-PGA-Ls in PBS, pH 7.4 at 37˚C. Each value represents the mean ± S.D. (n=3). *p< 0.05.

3.6 *In vitro* cytotoxic assay of liposomes

Next, the cytotoxicities of TEA-PGA-Ls were evaluated in LLC cells by 48 h exposure (Fig. 16). TEA-L and AS-L showed lower cytotoxicity (0.6 and 0.9 μg/mL, respectively) than DOX solution (0.05 μg/mL) (Fig. 16-A). Irrespective of the PGA molecular weight (Fig. 16-B) or PGA concentrations (Fig. 16-C), the IC_{50} values of TEA-PGA-Ls (0.6–0.9 μg/mL) were almost the same as those of AS-L and TEA-L, which were approximately 18-fold lower than that of DOX solution. These results indicated that exposure of cells to

dosage forms such as liposomes or solution was more influenced by the *in vitro* cytotoxicity of DOX than the intraliposomal conditions.

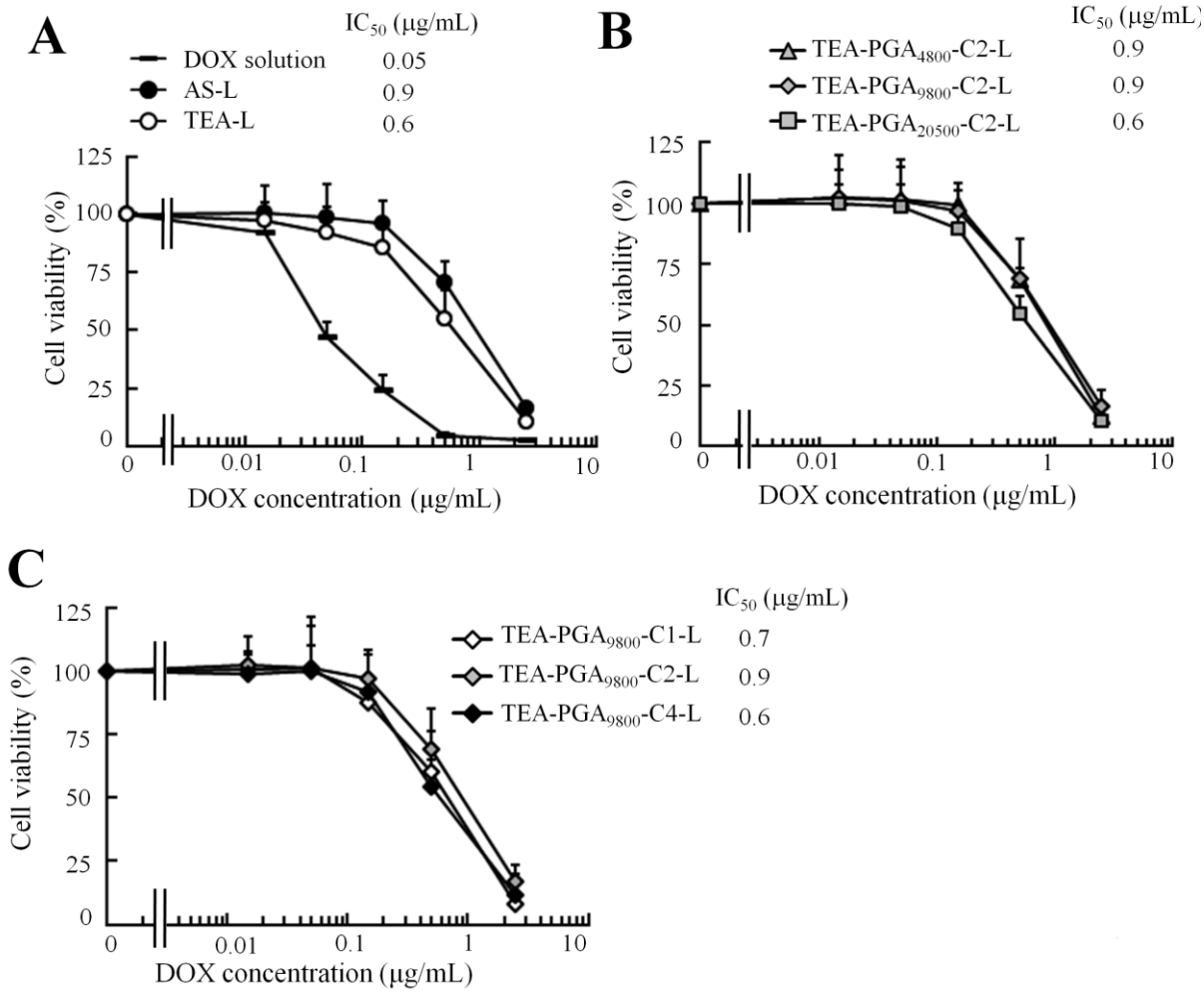

Figure 16. *In vitro* cytotoxicities of AS-L and TEA-L (A), and TEA-PGA-Ls (B and C) on LLC cells. AS-L and TEA-L (A), TEA-PGA-Ls prepared with PGA with molecular weights of 4800, 9800, or 20500 (B) or at various concentrations of PGA_{9800} (1, 2, or 4 mg/mL) (C) were added to the cells at various concentrations of DOX and then incubated for 48 h. Each value represents the mean ± S.D. (n=3).

3.7 Antitumor activity of liposomal DOX

The antitumor activity of TEA-PGA-Ls was evaluated in LLC tumor-bearing mice (Fig. 17). Compared with the injection of saline or DOX solution, a single injection of liposomal DOX could inhibit tumor growth up to day 8. Among the TEA-PGA-Ls prepared with different molecular weights of PGA (Fig. 17-A) or concentrations of PGA (Fig. 17-B), TEA-PGA_{20500}-C2-L or TEA-PGA_{9800}-C4-L strongly inhibited tumor growth similar to AS-L. No body weight change was observed during the period of the experiment (Fig. 17-C).

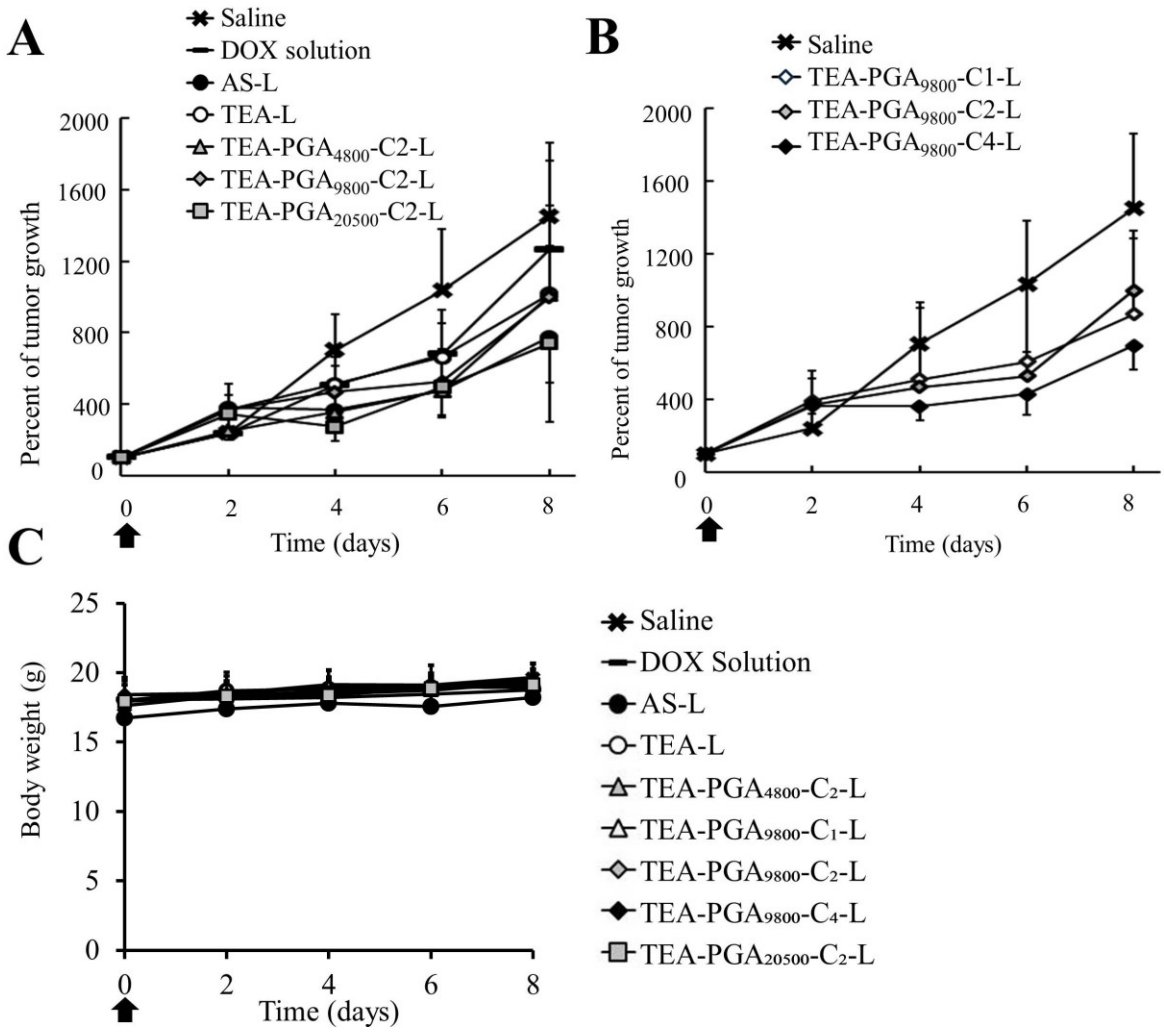

Figure 17. The antitumor activity of TEA-PGA-Ls on LLC tumor-bearing mice. TEA-PGA-Ls prepared with PGA with molecular weights of 4800, 9800, or 20500 at 2 mg/mL (A) or at various concentrations of PGA_{9800} (1, 2, or 4 mg/mL) (B) were administered by a single intravenous injection of 5 mg DOX per kg on day 0 (as indicated by black arrows). The body weights were evaluated at days post treatment (C). Each value represents the mean ± S.D. (n=3-4).

3.8 Biodistribution of liposomal DOX

Finally, the biodistribution of liposomal DOX at 24 h after intravenous injection was evaluated in LLC tumor-bearing mice (Fig. 18). Compared with DOX solution, which was almost cleared from the systemic circulation (0.6% of the injected dose remained at 24 h), TEA-PGA-Ls remained in serum at 10–15% of the injected dose at 24 h (Fig. 18-A). Higher tumor accumulation of DOX was observed in TEA-PGA_{9800}-C4-L and AS-L than TEA-PGA_{4800}-C2-L or TEA-PGA_{9800}-C2-L (Fig. 18-B). This suggested that TEA-PGA-Ls prepared with a high concentration of PGA could improve tumor accumulation of DOX by prolonged circulation in the bloodstream (EPR effect). The accumulation of DOX in the liver and spleen after injection of TEA-PGA-Ls and AS-L was higher than that of DOX solution (Figs. 18-C,D). In contrast, the accumulation of DOX in kidneys, lung, and heart after injection of DOX solution, AS-L, or TEA-PGA-Ls was low and did not show significantly differences between them (Figs. 18-E-G).

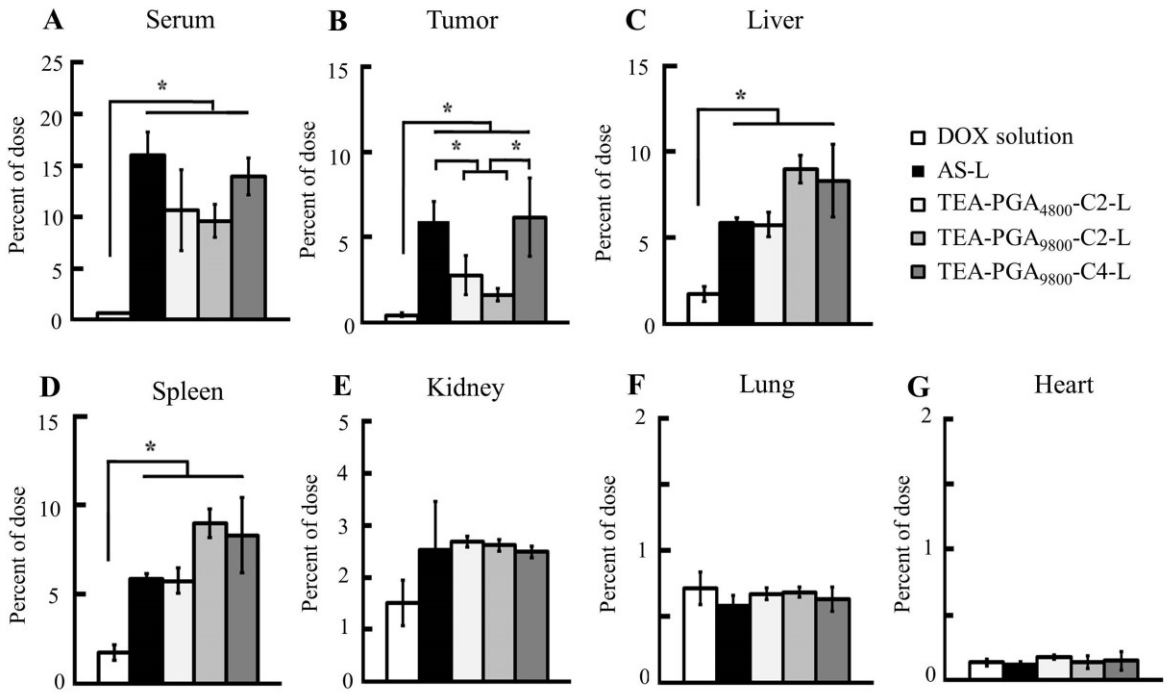

Figure 18. The biodistribution of DOX in LLC tumor-bearing mice at 24 h after a single intravenous injection of DOX solution, AS-L and TEA-PGA-Ls at doses equal to 5 mg DOX per kg. Each value represents the mean ± S.D. (n=4). *$p < 0.05$.

IV. DISCUSSION

Preparation of liposomes with high and stable drug loading is a promising strategy to enhance the antitumor effect by EPR. In this study, TEA-PGA-Ls were prepared using anionic PGA as an intraliposomal trapping agent that electrostatically interacted with cationic DOX inside liposomes. As a result, TEA-PGA-Ls prepared with high molecular weight or high concentration of PGA could efficiently accumulate DOX in tumors and strongly inhibit tumor growth in LLC tumor-bearing mice, which were similar to those of AS-L prepared using an AS gradient.

Poly-γ-glutamic acid has many carboxyl groups on its polymeric structure, which can be ionized at around pH 7 and provide useful sites for interactions with cationic drugs, such as DOX.[51] In this study, PGA was studied for preparing liposomal DOX instead of poly-γ-glutamic acid. When the solution of PGA was mixed with DOX solution, water insoluble-like aggregates of different sizes and densities of aggregates were observed depending on the molar ratio of DOX to PGA (Fig. 12). Furthermore, reduction of DOX release from liposomes was observed in TEA-PGA-Ls compared with TEA-L that did not contain PGA (Fig. 15). Although the details of DOX association with PGA in liposomes could not be clarified, it was speculated that the physicochemical interaction between PGA and DOX may occur in more stable conditions by raising the number of carboxyl group of L-glutamic acid either by increasing the concentration or length of PGA. It has been reported that the interaction of poly-γ-glutamic acid and DOX does not only involve ionic interactions between the amine group of DOX and carboxyl group of poly-γ-glutamic acid, but also hydrophobic interaction between the anthracycline ring of DOX and the hydrophobic domains of the polymer.[51] Furthermore, we observed a pH-dependent release of DOX from PGA/DOX aggregates (Fig. 14). It has been reported that the pKa value of PGA was 5.4.[50] Therefore, protonation of the

carboxyl group in PGA at pH 5.5 might result in the dissociation of DOX from DOX/PGA aggregates.

In the case of AS gradient method, beside DOX precipitation occurring as the result of over-solubility limits, the formation of DOX-sulfate gel increased drug retention inside the liposomes.[45,85] However, it has been reported that these precipitates of DOX are bioavailable, which means the DOX can be released from liposomes.[86] From the results of *in vitro* cytotoxicity assays against LLC cells, the cytotoxicity of TEA-PGA-Ls was similar to that of AS-L (Fig. 16), indicating that DOX entrapped in TEA-PGA-Ls could also be bioavailable to produce toxic effects on tumor cells.

The TEA-PGA-Ls prepared with high molecular weight or high concentration of PGA showed similar profiles of cytotoxicity, biodistribution, and antitumor activity, compared with those of AS-Ls. However, the aggregates of PGA/DOX had different physical characteristics from the aggregates of DOX produced by addition of AS (Fig. 12). On the other hand, the identical patterns of SAXRD profiles of AS-L, TEA-L and TEA-PGA-Ls at scattering vector (q) between 0.06 - 0.6 $Å^{-1}$ (Fig. 13) indicate that PGA-TEA-Ls and AS-L exist as vesicles [87,88]. But, the difference of scattering intensities observed at q below 0.05 $Å^{-1}$ between TEA-PGA-Ls and AS-L revealed that DOX/PGA aggregates filled in inner phase of TEA-PGA-Ls were dissimilar in shape with DOX aggregates in AS-L.[89] It has been reported that interaction of DOX with sulfate produced aggregation inside liposomes in the form of one-dimensional rods, which forced the vesicle shape to change from spherical to non-spherical.[41] In addition, the addition of PGA into TEA-L increased the scattering intensity (Fig. 13), which suggests that TEA-PGA-Ls are spherical vesicles with DOX/PGA aggregates in inner phase. However, further study must be performed to investigate the physical characteristics of PGA/DOX aggregates in liposomes.

In this study, all TEA-PGA-Ls could enhance the antitumor activity of DOX in LLC tumor-bearing mice until day 8 after only a single drug injection, compared with DOX solution. This could be due to the successful delivery of TEA-PGA-Ls to the tumor tissue by EPR effects. In EPR effects, maintaining a high drug concentration in the blood can have substantial impact on drug exposure of tumor tissues.[75,90] As shown in Fig. 18, DOX concentration in the serum at 24 h after administration of TEA-PGA-Ls was approximately 16–25-fold higher than that of DOX solution, but a high accumulation of DOX in tumors was observed after injection of TEA-PGA_{9800}-C4-L. Unstable drug entrapment can cause premature drug release from liposomes in systemic circulation, resulting lower amounts of liposomal drug accumulated in tumor tissue.[91,92] These findings indicated that DOX was stably entrapped in TEA-PGA-Ls, circulated for a prolonged time in the systemic blood, and accumulated in tumors.

The use of PGA as an intraliposomal trapping agent could improve tumor delivery of liposomal DOX. Unstable drug entrapment in liposomes causes rapid release of the drug, thus reducing the benefits of liposomal formulation. Excessive slow drug release will compromise therapeutic activity of the entrapped drug, because it will produce an inadequate drug concentration. It is important to tailor drug delivery for deliberate release of the drug in an appropriate manner in order to achieve high antitumor activity. However, further investigation is still required to evaluate the physicochemical properties of the aggregates of DOX and PGA for enhancing the therapeutic outcomes of TEA-PGA-Ls.

CONCLUSION

The complex system that occurs inside tumor has been challenging for drug delivery. Tumor microenvironment, which involves the interaction among cancer cells and between cancer cells with others, creates barriers that are responsible for drug transport and penetration of liposomal DOX to tumor tissue. Moreover, since liposomal DOX are exposed to many physiological barriers before finally reaching cancer cells during its distribution throughout the body, the stability of liposomal DOX importantly affect delivery of DOX. These factors should be considered for ensuring that the concentration of DOX is adequate and pharmacologically effective for chemotherapy. These present works revealed that modulation of tumor microenvironment by ZOL treatment and preparation of stable liposomes with PGA could enhance tumor delivery of DOX.

Managing tumor microenvironment by ZOL treatments provided an alternative approach to increase the antitumor effect of liposomal DOX. Irregularity and sprouting of tumor neovasculatures produce non-homogenous distribution of DOX inside tumor, where most of liposomes could only be transported into area near blood vessels. Moreover, IFP prevents liposome to further penetrate into deeper tumor site. As the consequences, liposomal drug is preferentially accumulated only in peripheral area of tumor, and its concentration in the core of tumor tissue tends to be inadequate for effective killing of cancer cells. Therefore, viable cancer cells are still exist and could promote cancer progression. ZOL treatment could decrease density of narrow vessels, which increased tumor blood flow and produced normalization of tumor vasculatures. The effect of ZOL on TAMs depletion has also contributed to reduction of tumor neovascularization, thus further promoted normalization of elevated IFP in tumor tissue. Although ZOL injections did not significantly increase the tumor accumulation of DOX, the antitumor activity of liposomal DOX was shown to be

increased in mice bearing subcutaneous LLC tumor. These results suggested that ZOL treatments might increase the therapeutic efficacy of liposomal DOX *via* improvement of DOX distribution in tumor by changing the tumor vasculatures. Moreover, the reduction of liposomal uptake by Kupffer cells in liver that improved the amount of liposomal DOX circulated in serum might also responsible for its enhanced antitumor activity.

It was shown that PGA could act as an excellent trapping agent for stable liposomal carriers. Tailoring stable liposome is important to minimize non-tumor specific release of DOX during biodistribution. Beside it could impede the toxic effects of DOX to healthy organs; it also could avoid huge drug loss ensuring the sufficient amount of drug could be delivered to tumor. TEA-PGA-Ls prepared with a high concentration of PGA could enhance DOX accumulation in tumors and prolonged DOX circulation in the serum, indicating that DOX may be stably retained in the liposomal interior by interaction with PGA. Furthermore, injection of TEA-PGA-liposomes prepared with the highest PGA concentration (4 mg/mL PGA_{9800}) or molecular weight (2 mg/mL PGA_{20500}) strongly inhibited tumor growth in LLC tumor-bearing mice. These results showed that the more stable the DOX and PGA interaction in liposomes, the more effective the tumor delivery of DOX would be achieved.

In conclusion, the stable liposomal DOX, which was achieved by intraliposomal trapping agent with PGA, gave benefits for reduction of drug loss in the bloodstream during drug administration in the body. It resulted in high amount of DOX entrapped in liposome that is highly required for further accumulation in tumor. The ZOL effects on macrophage depletion further enhanced prolonging time for the intact liposomes to be distributed into tumor. The improved tumor microenvironments by ZOL treatments, which are characterized by developed blood flow and decreased high tumor IFP, facilitated delivery of liposomal DOX. These works reveal that ZOL co-treatment and stable PGA-liposomal DOX could be effective ways to improve antitumor activity of DOX. Exploiting ZOL pretreatment and

stable liposomes prepared with PGA may lead to a new strategy for achieving high efficacy of antitumor drugs. The pH sensitive property and wide variety of molecular weights of PGA will be suitable for tailoring drug release aimed for tumor-specific delivery, while improving tumor vascularization and managing liposomal uptake by RES would give benefits for high tumor drug distribution.

ACKNOWLEDGMENTS

ALHAMDULILLAH, thanks to Allah SWT for His infinite blessings, that finally I could finish this dissertation. My deep appreciation and thanks to Hoshi University for providing me a prestigious scholarship during this work.

I would like first to thank my thesis advisors at the Department of Drug Delivery Research, Hoshi University: Firstly, to Prof. Hiraku Onishi, for his supportive guidance and helpful tutorship during my PhD study. Secondly, to Associate Prof. Yoshiyuki Hattori, for his great contributions to my research works and this dissertation, and also for the invaluable supports and opportunities he gave to me, so I could obtain wonderful experiences during my PhD study. And, special thanks to my research supervisor, Assistant Prof. Kumi Kawano, who was always open whenever I ran into a trouble spot or had a question about my research or writing. Thank you for consistently guiding my works and steering me in the right direction whenever I needed it.

I would also like to thank my former professors at Laboratory of Fine Drug Targeting of Hoshi University, who are Prof. Etsuo Yonemochi (Department of Physical Chemistry, Hoshi University) and Prof. Yoshie Maitani (Keio University). Many thanks for your support and invaluable intentions to my PhD works.

I thank my fellow lab mates: Takuto Kikuchi, Hitomi Yoda, Ai Fukasawa, Yoko Machida, Mari Nakamura, Nozomi Takeuchi, Yuuki Yoshiike, Keita Yamamoto, and Misaki Ikeda, for their supports in conducting researches, valuable discussions in my research works, and for all unforgettable moments in my life in Japan.

Last but not the least; I would like to thank all of my family for their continued support. Special thanks to my wife and my son, Ken, for the never ending supports over the last three years. I could not have done any of it without you all.

REFERENCES

1) Hanahan D, Weinberg RA. The hallmarks of cancer, Review. *Cell*, **100**, 57–70 (2000).
2) Vineis P, Wild CP. Global cancer patterns: Causes and prevention. *Lancet*, **383**, 549–557 (2014).
3) Balkwill FR, Capasso M, Hagemann T. The tumor microenvironment at a glance. *J. Cell Sci.*, **125**, 5591–5596 (2012).
4) Pérez-Herrero E, Fernández-Medarde A. Advanced targeted therapies in cancer: Drug nanocarriers, the future of chemotherapy. *Eur. J. Pharm. Biopharm.*, **93**, 52–79 (2015).
5) DeVita VT, Chu E. A history of cancer chemotherapy. *Cancer Res.*, **68**, 8643–8653 (2008).
6) Kemp JA, Shim MS, Heo CY, Kwon YJ. "Combo" nanomedicine: Co-delivery of multi-modal therapeutics for efficient, targeted, and safe cancer therapy. *Adv. Drug Deliv. Rev.*, **98**, 3–18 (2016).
7) Chastagner P, Sudour H, Mriouah J, Barberi-Heyob M, Bernier-Chastagner V, Pinel S. Preclinical studies of Pegylated- and non-Pegylated liposomal forms of doxorubicin as radiosensitizer on orthotopic high-grade glioma xenografts. *Pharm. Res.*, **32**, 158–166 (2014).
8) Chabner BA, Roberts TG. Timeline: Chemotherapy and the war on cancer. *Nat. Rev. Cancer*, **5**, 65–72 (2005).
9) Goel S, Duda DG, Xu L, Munn LL, Boucher Y, Fukumura D, Jain RK. Normalization of the vasculature for treatment of cancer and other diseases. *Physiol. Rev.*, **91**, 1071–121 (2011).
10) Dudley AC. Tumor endothelial cells. *Cold Spring Harb. Perspect. Med.*, **2**, 1–18 (2012).
11) Torchilin V. Tumor delivery of macromolecular drugs based on the EPR effect. *Adv. Drug Deliv. Rev.*, **63**, 131–135 (2011).
12) Maeda H. Macromolecular therapeutics in cancer treatment: The EPR effect and beyond. *J. Control. Release*, **164**, 138–144 (2012).
13) Lian T, Ho RJ. Trends and developments in liposome drug delivery systems. *J. Pharm. Sci.*, **90**, 667–680 (2001).
14) Çağdaş M, Sezer AD, Bucak S. Liposomes as potential drug carrier systems for drug delivery. *Nanotechnology and Nanomaterials » "Application of Nanotechnology in Drug Delivery"*. pp.1–50 (2014).

15) Allen TM, Cullis PR. Liposomal drug delivery systems: From concept to clinical applications. *Adv. Drug Deliv. Rev.*, **65**, 36–48 (2013).
16) Lombardo D, Calandra P, Barreca D, Magazù S, Kiselev M. Soft interaction in liposome nanocarriers for therapeutic drug delivery. *Nanomaterials*, **6**, 125 (2016).
17) Schilt Y, Berman T, Wei X, Barenholz Y, Raviv U. Using solution X-ray scattering to determine the high-resolution structure and morphology of PEGylated liposomal doxorubicin nanodrugs. *Biochim. Biophys. Acta - Gen. Subj.*, **1860**, 108–119 (2016).
18) Volkova M, Russell III R. Anthracycline cardiotoxicity: Prevalence, pathogenesis and treatment. *Curr. Cardiol. Rev.*, **7**, 214–220 (2011).
19) Mohan P, Rapoport N. Doxorubicin as a molecular nanotheranostic agent: Effect of doxorubicin encapsulation in micelles or nanoemulsions on the ultrasound-mediated intracellular delivery and nuclear trafficking. *Mol. Pharm.*, **7**, 1959–1973 (2010).
20) Zhang S, Liu X, Bawa-Khalfe T, Lu L-S, Lyu YL, Liu LF, Yeh ETH. Identification of the molecular basis of doxorubicin-induced cardiotoxicity. *Nat. Med.*, **18**, 1639–1645 (2012).
21) Wang X, Li S, Shi Y, Chuan X, Li J, Zhong T, Zhang H, Dai W, He B, Zhang Q. The development of site-specific drug delivery nanocarriers based on receptor mediation. *J. Control. Release*, **193**, 139–153 (2014).
22) Ozcelikkale A, Ghosh S, Han B. Multifaceted transport characteristics of nanomedicine: Needs for characterization in dynamic environment. *Mol. Pharm.*, **10**, 2111–2126 (2013).
23) Munson JM, Shieh AC. Interstitial fluid flow in cancer: implications for disease progression and treatment. *Cancer Manag. Res.*, **6**, 317–28 (2014).
24) Ekdawi SN, Stewart JMP, Dunne M, Stapleton S, Mitsakakis N, Dou YN, Jaffray DA, Allen C. Spatial and temporal mapping of heterogeneity in liposome uptake and microvascular distribution in an orthotopic tumor xenograft model. *J. Control. Release*, **207**, 101–111 (2015).
25) Stapleton S, Milosevic M, Tannock IF, Allen C, Jaffray DA. The intra-tumoral relationship between microcirculation, interstitial fluid pressure and liposome accumulation. *J. Control. Release*, **211**, 163–170 (2015).
26) Trédan O, Galmarini CM, Patel K, Tannock IF. Drug resistance and the solid tumor microenvironment. *J. Natl. Cancer Inst.*, **99**, 1441–1454 (2007).
27) Shang B, Cao Z, Zhou Q. Progress in tumor vascular normalization for anticancer therapy: Challenges and perspectives. *Front. Med. China*, **6**, 67–78 (2012).

28) Jain RK. Normalizing tumor vasculature with anti-angiogenic therapy: a new paradigm for combination therapy. *Nat. Med.*, **7**, 987–989 (2001).

29) Huang D, Lan H, Liu F, Wang S, Chen X, Jin K, Mou X. Anti-angiogenesis or pro-angiogenesis for cancer treatment: Focus on drug distribution. *Int. J. Clin. Exp. Med.*, **8**, 8369–8376 (2015).

30) Pollard JW. Tumour-educated macrophages promote tumour progression and metastasis. *Nat. Rev. Cancer*, **4**, 71–78 (2004).

31) Condeelis J, Pollard JW. Macrophages: Obligate partners for tumor cell migration, invasion, and metastasis. *Cell*, **124**, 263–266 (2006).

32) Murdoch C, Muthana M, Coffelt SB, Lewis CE. The role of myeloid cells in the promotion of tumour angiogenesis. *Nat Rev Cancer*, **8**, 618–631 (2008).

33) Kobayashi N, Miyoshi S, Mikami T, Koyama H, Kitazawa M, Takeoka M, Sano K, Amano J, Isogai Z, Niida S, Oguri K, Okayama M, McDonald JA, Kimata K, Taniguchi S, Itano N. Hyaluronan deficiency in tumor stroma impairs macrophage trafficking and tumor neovascularization. *Cancer Res.*, **70**, 7073–7083 (2010).

34) Zhang W, Zhu XD, Sun HC, Xiong YQ, Zhuang PY, Xu HX, Kong LQ, Wang L, Wu WZ, Tang ZY. Depletion of tumor-associated macrophages enhances the effect of sorafenib in metastatic liver cancer models by antimetastatic and antiangiogenic effects. *Clin. Cancer Res.*, **16**, 3420–3430 (2010).

35) Rogers MJ, Gordon S, Benford HL, Coxon FP, Luckman SP, Monkkonen J, Frith JC. Cellular and molecular mechanisms of action of bisphosphonates. *Cancer*, **88**, 2961–2978 (2000).

36) Ross JR, Saunders Y, Edmonds PM, Patel S, Wonderling D, Normand C, Broadley K. A systematic review of the role of bisphosphonates in metastatic disease. *Health Technol. Assess.*, **8**, 1–176 (2004).

37) Thompson K, Rogers MJ, Coxon FP, Crockett JC. Cytosolic entry of bisphosphonate drugs requires acidification of vesicles after fluid-phase endocytosis. *Mol. Pharmacol.*, **69**, 1624–1632 (2006).

38) Ottewell PD, Monkkonen H, Jones M, Lefley D V., Coleman RE, Holen I. Antitumor effects of doxorubicin followed by zoledronic acid in a mouse model of breast cancer. *J. Natl. Cancer Inst.*, **100**, 1167–1178 (2008).

39) Andriyanov A V., Koren E, Barenholz Y, Goldberg SN. Therapeutic efficacy of combining PEGylated liposomal doxorubicin and radiofrequency (RF) ablation: Comparison between slow-drug-releasing, non-thermosensitive and fast-drug-releasing,

thermosensitive nano-liposomes. *PLoS One*, **9**, (2014).

40) Drummond DC, Meyer O, Hong K, Kirpotin DB, Papahadjopoulos D. Optimizing liposomes for delivery of chemotherapeutic agents to solid tumors. *Pharmacol. Rev.*, **51**, 691–743 (1999).

41) Barenholz Y. Doxil® - The first FDA-approved nano-drug: Lessons learned. *J. Control. Release*, **160**, 117–134 (2012).

42) Seynhaeve ALB, Dicheva BM, Hoving S, Koning GA, Ten Hagen TLM. Intact Doxil is taken up intracellularly and released doxorubicin sequesters in the lysosome: Evaluated by in vitro/in vivo live cell imaging. *J. Control. Release*, **172**, 330–340 (2013).

43) Cheung BCL, Sun THT, Leenhouts JM, Cullis PR. Loading of doxorubicin into liposomes by forming Mn2+-drug complexes. *Biochim. Biophys. Acta - Biomembr.*, **1414**, 205–216 (1998).

44) Hattori Y, Shi L, Ding W, Koga K, Kawano K, Hakoshima M, Maitani Y. Novel irinotecan-loaded liposome using phytic acid with high therapeutic efficacy for colon tumors. *J. Control. Release*, **136**, 30–37 (2009).

45) Lasic DD, Ceh B, Stuart MC, Guo L, Frederik PM, Barenholz Y. Transmembrane gradient driven phase transitions within vesicles: lessons for drug delivery. *Biochim. Biophys. Acta*, **1239**, 145–156 (1995).

46) Thomas AM, Kapanen AI, Hare JI, Ramsay E, Edwards K, Karlsson G, Bally MB. Development of a liposomal nanoparticle formulation of 5-Fluorouracil for parenteral administration: Formulation design, pharmacokinetics and efficacy. *J. Control. Release*, **150**, 212–219 (2011).

47) Drummond DC, Noble CO, Guo Z, Hong K, Park JW, Kirpotin DB. Development of a highly active nanoliposomal irinotecan using a novel intraliposomal stabilization strategy. *Cancer Res.*, **66**, 3271–3277 (2006).

48) Zhigaltsev I V., Maurer N, Akhong QF, Leone R, Leng E, Wang J, Semple SC, Cullis PR. Liposome-encapsulated vincristine, vinblastine and vinorelbine: A comparative study of drug loading and retention. *J. Control. Release*, **104**, 103–111 (2005).

49) Zucker D, Andriyanov A V., Steiner A, Raviv U, Barenholz Y. Characterization of PEGylated nanoliposomes co-remotely loaded with topotecan and vincristine: Relating structure and pharmacokinetics to therapeutic efficacy. *J. Control. Release*, **160**, 281–289 (2012).

50) Abbruzzetti S, Viappiani C, Small JR, Libertini LJ, Small EW. Kinetics of local helix formation in poly-L-glutamic acid studied by time-resolved photoacoustics:

neutralization reactions of carboxylates in aqueous solutions and their relevance to the problem of protein folding. *Biophys. J.*, **79**, 2714–2721 (2000).

51) Margaritis A, Manocha B. Controlled release of doxorubicin from doxorubicin/γ-polyglutamic acid ionic complex. *J. Nanomater.*, **2010**, 1–9 (2010).

52) Kaminska K, Szczylik C, Bielecka ZF, Bartnik E, Porta C, Lian F, Czarnecka AM. The role of the cell-cell interactions in cancer progression. *J. Cell. Mol. Med.*, **19**, 283–296 (2015).

53) Marcucci F, Corti A. How to improve exposure of tumor cells to drugs - Promoter drugs increase tumor uptake and penetration of effector drugs. *Adv. Drug Deliv. Rev.*, **64**, 53–68 (2012).

54) Kano MR, Bae Y, Iwata C, Morishita Y, Yashiro M, Oka M, Fujii T, Komuro A, Kiyono K, Kaminishi M, Hirakawa K, Ouchi Y, Nishiyama N, Kataoka K, Miyazono K. Improvement of cancer-targeting therapy, using nanocarriers for intractable solid tumors by inhibition of TGF-beta signaling. *Proc. Natl. Acad. Sci. U. S. A.*, **104**, 3460–3465 (2007).

55) Taniguchi Y, Kawano K, Minowa T, Sugino T, Shimojo Y, Maitani Y. Enhanced antitumor efficacy of folate-linked liposomal doxorubicin with TGF-β type I receptor inhibitor. *Cancer Sci.*, **101**, 2207–2213 (2010).

56) Batchelor TT, Sorensen AG, di Tomaso E, Zhang WT, Duda DG, Cohen KS, Kozak KR, Cahill DP, Chen PJ, Zhu M, Ancukiewicz M, Mrugala MM, Plotkin S, Drappatz J, Louis DN, Ivy P, Scadden DT, Benner T, Loeffler JS, Wen PY, Jain RK. AZD2171, a pan-VEGF receptor tyrosine kinase inhibitor, normalizes tumor vasculature and alleviates edema in glioblastoma patients. *Cancer Cell*, **11**, 83–95 (2007).

57) Hattori Y, Yamashita J, Sakaida C, Kawano K, Yonemochi E. Evaluation of antitumor effect of zoledronic acid entrapped in folate-linked liposome for targeting to tumor-associated macrophages. *J. Liposome Res.*, **25**, 1–10 (2014).

58) Kato M, Hattori Y, Kubo M, Maitani Y. Collagenase-1 injection improved tumor distribution and gene expression of cationic lipoplex. *Int. J. Pharm.*, **423**, 428–434 (2012).

59) Ogawara K-I, Un K, Minato K, Tanaka K-I, Higaki K, Kimura T. Determinants for in vivo anti-tumor effects of PEG liposomal doxorubicin: importance of vascular permeability within tumors. *Int. J. Pharm.*, **359**, 234–40 (2008).

60) Santini D, Vincenzi B, Dicuonzo G, Avvisati G, Massacesi C, Battistoni F, Gavasci M, Rocci L, Tirindelli MC, Altomare V, Tocchini M, Bonsignori M, Tonini G. Zoledronic

acid induces significant and long-lasting modifications of circulating angiogenic factors in cancer patients. *Clin. Cancer Res.*, **9**, 2893–2897 (2003).

61) Giraudo E, Inoue M, Hanahan D. An amino-bisphosphonate targets MMP-9 - Expressing macrophages and angiogenesis to impair cervical carcinogenesis. *J. Clin. Invest.*, **114**, 623–633 (2004).

62) Wood J, Bonjean K, Ruetz S, Bellahcène A, Devy L, Foidart JM, Castronovo V, Green JR. Novel antiangiogenic effects of the bisphosphonate compound zoledronic acid. *J. Pharmacol. Exp. Ther.*, **302**, 1055–61 (2002).

63) Corso A, Ferretti E, Lazzarino M. Zoledronic acid exerts its antitumor effect in multiple myeloma interfering with the bone marrow microenvironment. *Hematology*, **10**, 215–224 (2005).

64) Bezzi M, Hasmim M, Bieler G, Dormond O, Ruegg C. Zoledronate sensitizes endothelial cells to tumor necrosis factor-induced programmed cell death: evidence for the suppression of sustained activation of focal adhesion kinase and protein kinase B/Akt. *J Biol Chem*, **278**, 43603–43614 (2003).

65) Dicuonzo G, Vincenzi B, Santini D, Avvisati G, Rocci L, Battistoni F, Gavasci M, Borzomati D, Coppola R, Tonini G. Fever after zoledronic acid administration is due to increase in TNF-alpha and IL-6. *J Interf. Cytokine Res*, **23**, 649–654 (2003).

66) Tanvetyanon T, Stiff PJ. Management of the adverse effects associated with intravenous bisphosphonates. *Ann. Oncol.*, **17**, 897–907 (2006).

67) Reid IR, Gamble GD, Mesenbrink P, Lakatos P, Black DM. Characterization of and risk factors for the acute-phase response after zoledronic acid. *J. Clin. Endocrinol. Metab.*, **95**, 4380–4387 (2010).

68) Clezardin P, Massaia M. Nitrogen-containing bisphosphonates and cancer immunotherapy. *Curr Pharm Des*, **16**, 2014–3007 (2010).

69) Coscia M, Quaglino E, Iezzi M, Curcio C, Pantaleoni F, Riganti C, Holen I, Mönkkönen H, Boccadoro M, Forni G, Musiani P, Bosia A, Cavallo F, Massaia M. Zoledronic acid repolarizes tumour-associated macrophages and inhibits mammary carcinogenesis by targeting the mevalonate pathway. *J. Cell. Mol. Med.*, **14**, 2803–2815 (2010).

70) Riganti C, Castella B, Kopecka J, Campia I, Coscia M, Pescarmona G, Bosia A, Ghigo D, Massaia M. Zoledronic acid restores doxorubicin chemosensitivity and immunogenic cell death in multidrug-resistant human cancer cells. *PLoS One*, **8**, 1–16 (2013).

71) Yoshizawa Y, Ogawara KI, Fushimi A, Abe S, Ishikawa K, Araki T, Molema G,

Kimura T, Higaki K. Deeper penetration into tumor tissues and enhanced in vivo antitumor activity of liposomal paclitaxel by pretreatment with angiogenesis inhibitor SU5416. *Mol. Pharm.*, **9**, 3486–3494 (2012).

72) Ohara Y, Oda T, Yamada K, Hashimoto S, Akashi Y, Miyamoto R, Kobayashi A, Fukunaga K, Sasaki R, Ohkohchi N. Effective delivery of chemotherapeutic nanoparticles by depleting host Kupffer cells. *Int. J. Cancer*, **131**, 2402–2410 (2012).

73) Ottewell PD, Brown HK, Jones M, Rogers TL, Cross SS, Brown NJ, Coleman RE, Holen I. Combination therapy inhibits development and progression of mammary tumours in immunocompetent mice. *Breast Cancer Res. Treat.*, **133**, 523–536 (2012).

74) Soundararajan A, Bao A, Phillips WT, Perez R, Goins BA. [186Re]Liposomal doxorubicin (Doxil): in vitro stability, pharmacokinetics, imaging and biodistribution in a head and neck squamous cell carcinoma xenograft model. *Nucl. Med. Biol.*, **36**, 515–524 (2009).

75) Dawidczyk CM, Kim C, Park JH, Russell LM, Lee KH, Pomper MG, Searson PC. State-of-the-art in design rules for drug delivery platforms: Lessons learned from FDA-approved nanomedicines. *J. Control. Release*, **187**, 133–144 (2014).

76) Tsukioka Y, Matsumura Y, Hamaguchi T, Koike H, Moriyasu F, Kakizoe T. Pharmaceutical and biomedical differences between micellar doxorubicin (NK911) and liposomal doxorubicin (Doxil). *Jpn. J. Cancer Res.*, **93**, 1145–1153 (2002).

77) Hattori Y, Shi L, Ding W, Koga K, Kawano K, Hakoshima M, Maitani Y. Novel irinotecan-loaded liposome using phytic acid with high therapeutic efficacy for colon tumors. *J. Control. Release*, **136**, 30–37 (2009).

78) Nickels JD, Perticaroli S, Ehlers G, Feygenson M, Sokolov AP. Rigidity of poly-L-glutamic acid scaffolds: Influence of secondary and supramolecular structure. *J. Biomed. Mater. Res. Part A*, **103**, 2909–2918 (2015).

79) Otani Y, Tabata Y, Ikada Y. A new biological glue from gelatin and poly(L-glutamic acid). *J. Biomed. Mater. Res.*, **31**, 157–166 (1996).

80) Tansey W, Ke S, Cao XY, Pasuelo MJ, Wallace S, Li C. Synthesis and characterization of branched poly(L-glutamic acid) as a biodegradable drug carrier. *J. Control. Release*, **94**, 39–51 (2004).

81) Sheff D. Endosomes as a route for drug delivery in the real world. *Adv. Drug Deliv. Rev.*, **56**, 927–930 (2004).

82) Dicko A, Tardi P, Xie X, Mayer L. Role of copper gluconate / triethanolamine in irinotecan encapsulation inside the liposomes. *Int. J. Pharm.*, **337**, 219–228 (2007).

83) Konarev P V., Volkov V V., Sokolova A V., Koch MHJ, Svergun DI. PRIMUS: A Windows PC-based system for small-angle scattering data analysis. *J. Appl. Crystallogr.*, **36**, 1277–1282 (2003).

84) Drummond DC, Noble CO, Guo Z, Hayes ME, Connolly-Ingram C, Gabriel BS, Hann B, Liu B, Park JW, Hong K, Benz CC, Marks JD, Kirpotin DB. Development of a highly stable and targetable nanoliposomal formulation of topotecan. *J. Control. Release*, **141**, 13–21 (2010).

85) Haran G, Cohen R, Bar LK, Barenholz Y. Transmembrane ammonium sulfate gradients in liposomes produce efficient and stable entrapment of amphipathic weak bases. *Biochim. Biophys. Acta*, **1151**, 201–215 (1993).

86) Horowitz AT, Barenholz Y, Gabizon AA. In vitro cytotoxicity of liposome-encapsulated doxorubicin: dependence on liposome composition and drug release. *Biochim. Biophys. Acta*, **1109**, 203–209 (1992).

87) Brzustowicz MR, Brunger AT. X-ray scattering from unilamellar lipid vesicles. *J. Appl. Crystallogr.*, **38**, 126–131 (2005).

88) Kucerka N, Tristram-Nagle S, Nagle JF. Structure of fully hydrated fluid phase lipid bilayers with monounsaturated chains. *J. Membr. Biol.*, **208**, 193–202 (2006).

89) Hirai M, Kimura R, Takeuchi K, Hagiwara Y, Kawai-Hirai R, Ohta N, Igarashi N, Shimuzu N. Structure of liposome encapsulating proteins characterized by X-ray scattering and shell-modeling. *J. Synchrotron Radiat.*, **20**, 869–874 (2013).

90) Bertrand N, Wu J, Xu X, Kamaly N, Farokhzad OC. Cancer nanotechnology: The impact of passive and active targeting in the era of modern cancer biology. *Adv. Drug Deliv. Rev.*, **66**, 2–25 (2014).

91) Fang J, Nakamura H, Maeda H. The EPR effect: Unique features of tumor blood vessels for drug delivery, factors involved, and limitations and augmentation of the effect. *Adv. Drug Deliv. Rev.*, **63**, 136–151 (2011).

92) Iyer AK, Khaled G, Fang J, Maeda H. Exploiting the enhanced permeability and retention effect for tumor targeting. *Drug Discov. Today*, **11**, 812–818 (2006).